Bifurcation and synchronization in parametrically forced systems

Hironori Kumeno

▶ **To cite this version:**

Hironori Kumeno. Bifurcation and synchronization in parametrically forced systems. Automatic Control Engineering. INSA de Toulouse, 2012. English. NNT : . tel-00749690

HAL Id: tel-00749690
https://theses.hal.science/tel-00749690

Submitted on 8 Nov 2012

HAL is a multi-disciplinary open access archive for the deposit and dissemination of scientific research documents, whether they are published or not. The documents may come from teaching and research institutions in France or abroad, or from public or private research centers.

L'archive ouverte pluridisciplinaire **HAL**, est destinée au dépôt et à la diffusion de documents scientifiques de niveau recherche, publiés ou non, émanant des établissements d'enseignement et de recherche français ou étrangers, des laboratoires publics ou privés.

Université de Toulouse

THÈSE

En vue de l'obtention du

DOCTORAT DE L'UNIVERSITÉ DE TOULOUSE

Délivré par :
Institut National des Sciences Appliquées de Toulouse (INSA de Toulouse)

Cotutelle internationale avec l'Université de Tokushima, Japon.

Présentée et soutenue par :
Hironori KUMENO

Le 24 septembre 2012

Titre :

Bifurcation and Synchronization in Parametrically Forced Systems

---

EDSYS : Automatique 4200046

Unité de recherche :
Laboratoire d'Analyse et d'Architecture des Systèmes

Directeur(s) de Thèse :

Danièle Fournier-Prunaret, Professeur INSA, France
Yoshifumi Nishio, Professeur à l'Université de Tokushima Japon

Rapporteurs :

René Lozi, Professeur à l'Université de Nice, France
Toshimichi Saito, Professeur à l'Université de Tokyo, Japon

Autre(s) membre(s) du jury :

Masaki Hashizume, Professeur à l'Université de Tokushima, Japon
Tesushi Ueta, Professeur à l'Université de Tokushima Japon
Ina Taralova, Maître de Conférences à l'Ecole Centrale de Nantes, France

Bifurcation and Synchronization in Parametrically Forced Systems

Dissertation Submitted
in Candidacy for
the Ph.D. Degree

by

Hironori KUMENO

September 2012

Contents

Chapter 1

General Introduction

1.1 Introduction

Coupled chaotic systems attract extensive attention as good models which describe the complicated phenomena in the natural world. The field of coupled chaotic systems has been developed since the discovering of synchronization of chaotic trajectories [1] and further analyzing of the synchronization [2]. Studies about the coupled systems are carried out in various field, such as in physics [3, 4], biology [5, 6] and engineering [7].

Furthermore, researchers suggest that synchronization phenomena of coupled systems have some relationships with information processing in brain. In the brain, information is processed by neurons. Due to control of the neurons by ion current, the neurons can have many states and execute processing of complex information despite of simpleness of neuron activity. When the neurons are forced by the ions, the behavior of the neurons are changed, thereby the neurons are possible to take many states. On the other hand, the system proposed in this study is a parametrically forced system. By the parametric force, steady states of the system are increased despite of absence of a force which directly perturb states of the system whereas parameters of the system are forced into periodic varying. Both of the neurons and the proposed system are controlled by the forces. By investigating such a forced system, we expect to observe interesting and complicated phenomena which are similar to those observed in the brain. We believe that investigation of synchronization phenomena of coupled systems does not only make progress on understanding of information processing mechanism of the brain, but also contributes to realize an information processing brain computer.

By the way, it has been reported that if an autonomic neuron is influenced by external force, its characteristics are changed such as the neuron behaves periodic or chaotic [15]. So, we expect that periodic external force can cause interesting phenomena. Especially, we focus

on a system whose parameter is forced into periodic varying and investigate behavior of the system and its coupling. Parametrically forced systems are still not investigated well, whereas systems whose state values are perturbed by external periodic waves are well investigated and many interesting and complicated phenomena are observed in the systems. The Duffing oscillator whose state value is perturbed by external sine wave is well known as a non-autonomous forced system and investigated and analyzed by many researchers. The parametric force almost causes periodic oscillation and chaos in a simple oscillator [16, 17, 18]. Previously, we have investigated coupled logistic maps whose parameters are forced into periodic varying and observed interesting characteristic behaviors of the parametrically forced system [20]. The aim of this study is to verify whether the behaviors observed in the discrete-time system we have investigated in the previous study can be observed in continuous-time systems.

In this thesis, we propose two kinds of coupled continuous-time systems whose parameters are forced into periodic varying, the coupled systems being constructed of n same one-dimensional subsystems with mutually influencing coupling and investigate bifurcations and synchronizations in the systems. This paper is organized as follows.

The next chapter is devoted to general background.

In chapter 3, we introduce a coupled parametrically forced discrete-time system in order to compare with the parametrically forced continuous-system in the latter chapter. We explain general properties of the parametrically forced discrete-time system, bifurcations and basins when logistic maps is used as the one-dimensional subsystem constructing the system.

In chapter 4, we propose a coupled Chua's circuit whose parameter is forced into periodic varying associated with the period of an internal state value and investigate behaviors by carrying out computer simulations and circuit experiments. From the investigation of bifurcations in the system, non-existence of odd order cycles and coexistence of different attractors are observed. Then, we investigate synchronizations in the coupled parametrically forced Chua's circuits. Coexisting of many attractors whose synchronizations states are different are observed. Furthermore, two kinds of shift of synchronization states are observed in thee-dimensional coupled case. Finally, observed phenomena in the system is compared with a parametrically forced discrete-time system. Similar phenomena are confirmed between the parametrically forced discrete-time system and the parametrically forced Chua's circuit.

In chapter 5, we investigate behaviors of the coupled parametrically forced Chua's circuits

explained in the previous chapter, although the motion of the switches controlling R is different from the switches in the previous chapter. Coexisting of many attractors whose synchronizations states are different are observed.

The last chapter is devoted to the conclusion.

Chapter 2

General Background

2.1 Discrete-Time System

2.1.1 Introduction

Let $T[X \rightarrow F(X, Lambda)]$ be a real map, X being a vector $(dimX = n)(X = (x_1, \ldots, x_n)), (F = (f_1, \ldots, f_n))$ and Λ an m-dimensional parameter $(\Lambda = (\lambda_1, \ldots, \lambda_m), \lambda_i \in R, i = 1, \ldots, m)$. F is assumed to be a smooth function of its arguments. A cycle (or periodic point) of order k of T is made up of k consequent points satisfying: $X = T^k X, X \neq T^l X, l < k$; l and k being integers.

With a cycle of order (or period) k are associated n multipliers $S_i (i = 1, \ldots, n)$ which are the eigenvalues of the Jacobian matrix $\partial F_k / \partial X$ (F_k being the k-iterated function from F; F_k defines T^k). Knowledge of the multipliers permits the characterization of the nature and the stability of the considered cycle.

A cycle of T is designated as a $(k; j)$ cycle where k is the order of the cycle and j differentiates cycles of the same order.

So, in the case where $n = 1$, a cycle possesses only one multiplier S and is said to be stable (or attractive) if $|S| < 1$, and unstable (or repulsive) if $|S| > 1$.

In the case where $n = 2$, a cycle having two multipliers S_1 and S_2, different kinds of cycles can be defined.

2.1.2 Coupling System

n-dimensional coupled system is constructed of n subsystems, which are one-dimensional maps, with a coupling scheme. As the coupling scheme, there are two basic scheme which are coupling map lattice (CML) and global coupling map (GCM). In CML, a subsystem is locally coupled to some of the other subsystems. For a basic coupling of CML, the coupling whose

subsystems are coupled to neighbor subsystems is considered and its system is described as,

$$x_p(n+1) = (1-\varepsilon)F(x_p(n)) + \frac{\varepsilon}{2}\left\{f(x_{p-1}(n)) + f(x_{p+1}(n))\right\}. \tag{2.1}$$

In GCM, a subsystem are coupled to all the other subsystems and its system is described as,

$$x_p(n+1) = (1-\varepsilon)F(x_p(n)) + \frac{\varepsilon}{N} \sim_{j=1}^{N} f(x_j(n)). \tag{2.2}$$

ε is coupling intensity and correspond to rate of influence weight between a considered subsystem and its coupled subsystems. The state value at any subsystems is mapped recursively with respect to itself and the coupled subsystems.

In this study, we treat a system with the coupling scheme of GCM.

2.1.3 Basic Bifurcation

2.1.3.1 Fold, flip pitchfork and neimark-sacker bifurcation

For given values of parameters $\lambda_i (i = 3, \ldots, m)$, different kinds of bifurcation curves can be obtained in the (λ_1, λ_2) parameter plane.

The fundamental bifurcations are the following ones [21, 22]:

Fold bifurcation $The fold bifurcation$ (in the simplest case, generation or extinction of a couple of cycles of order k):

$$\emptyset \leftrightarrow (k;j)node(s \text{ or } u) + (k;j)saddle, \tag{2.3}$$

where s means stable and u means unstable and $\emptyset$ indicates that there is no $(k;j)$ cycle in the neighborhood where the considered cycles appear. This kind of bifurcation occurs when one of the multipliers is unity. In the (λ_1, λ_2) parameter plane, a locus of such a bifurcation is a $foldbifurcationcurve$ noted $\Lambda^j_{(k)_0}$.

Flip bifurcation $The flip bifurcation$ (period doubling bifurcation); in the simplest case one has:

$$(k;j)node(s \text{ or } u) \leftrightarrow (k;j)saddle + (k.2^1;j)node(s \text{ or } u); \tag{2.4}$$

this kind of bifurcation occurs when one of the multipliers passes through the point (-1, 0) in the complex plane. In the (λ_1, λ_2) parameter plane, a locus of such a bifurcation is a $flipbifurcationcurve$ noted Λ^j_k.

Pitchfork bifurcation $The pitchfork bifurcation$; in the simplest case one has:

$$\begin{aligned} &(k;j)node \leftrightarrow (k;j)saddle + (k;j')node + (k;j")node \\ &(k;j)saddle \leftrightarrow (k;j)node + (k;j')saddle + (k;j")saddle; \end{aligned} \tag{2.5}$$

this kind of bifurcation occurs when one of the multipliers passes through the point (+1, 0) in the complex plane. In the (λ_1, λ_2) parameter plane, a locus of such a bifurcation is a $pitchforkbifurcationcurve$ noted $\bar{\Lambda}^j_{(k)_0}$.

Neimark-sacker bifurcation $TheNeimark-sackerbifurcation$; in the simplest case one has:

$$(k;j)focus(s \text{ or } u) \leftrightarrow (k;j)focus(s \text{ or } u) + ICC(s \text{ or } u), \tag{2.6}$$

where ICC indicates an invariant closed curve of T^k. This kind of bifurcation occurs when a pair of complex multipliers pass through the unit circle, except for (-1, 0) and (+1, 0). In the (λ_1, λ_2) a locus of such a bifurcation is a $Neimark-sacherbifurcation$ noted Γ^j_k.

2.1.3.2 Communication areas

In the (λ_1, λ_2) plane, a given point is generally related to different cycles $(k;j)$ with possibly different stability properties. Hence, this plane can be considered as "foliated" (foliated is here used in the sense of [23] and [24]) and made up of sheets, each corresponding to a given cycle or other singularities (Cantor set, invariant close curve.) A sheet may be bounded by fold and flip bifurcation curves, and also by Γ^j_k curves.

Communications between sheets are possible via singularities of codimension greater or equal to 1. The flip and fold bifurcation curves are codimension-1 singularities.

The only codimension-2 singularities what we consider are cusp points of fold bifurcation curves which involve the existence of k roots with multiplicity $q = 3$ for $X = T^k X$. In [21], necessary and sufficient conditions for the existence of a cusp point are given.

In the case of a cusp point, the communication between sheets of the parameter plane is defined by considering the flip bifurcation curves associated with the two branches of the considered cusp point. According to the association obtained, three fundamental bifurcation structures (also called communication areas) can be defined in the (λ_1, λ_2) plane: the crossroad area (CRA) (Fig. 2.1), the saddle area (SAA) (Fig. 2.2) and the spring area (SPA) (Fig. 2.3) [25, 26, 27]. It is worthy of note that certain CRA are defined from fold, flip and Γ^j_k curves [28].

2.1.4 Phase Plane

2.1.4.1 Basin

Basin D is the domain of influence or domain of attraction of an attracting set, i.e. open domain of the initial conditions generating a sequence of iterations (or iterated sequences)

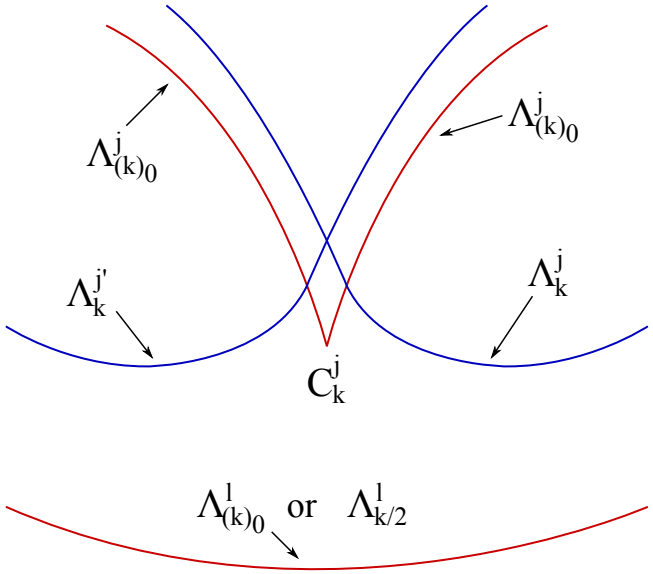

Figure 2.1 Parameter plane representation of a crossroad area related to a cusp point C_k^j and involving cycles of order k.

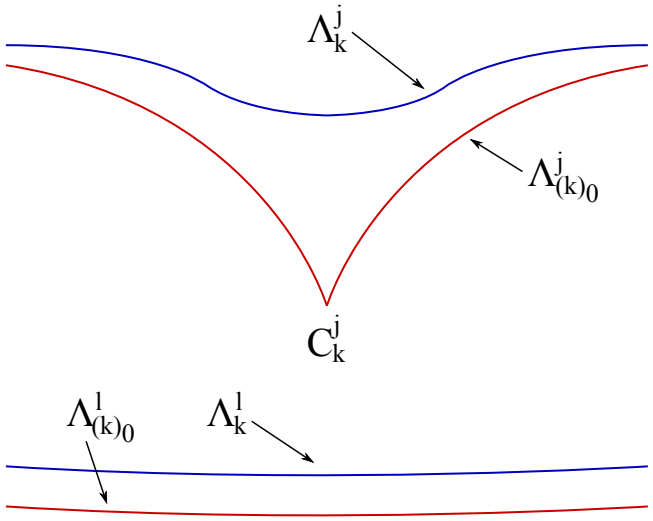

Figure 2.2 Parameter plane representation of a saddle area related to a cusp point C_k^j and involving cycles of order k.

converging toward a given attracting set A when the iterates rank tends toward infinity. D is invariant under backward iteration T^{-1} of T, but not necessarily invariant by T:

$$T^{-1}(D) = D, T(D) \subseteq D. \tag{2.7}$$

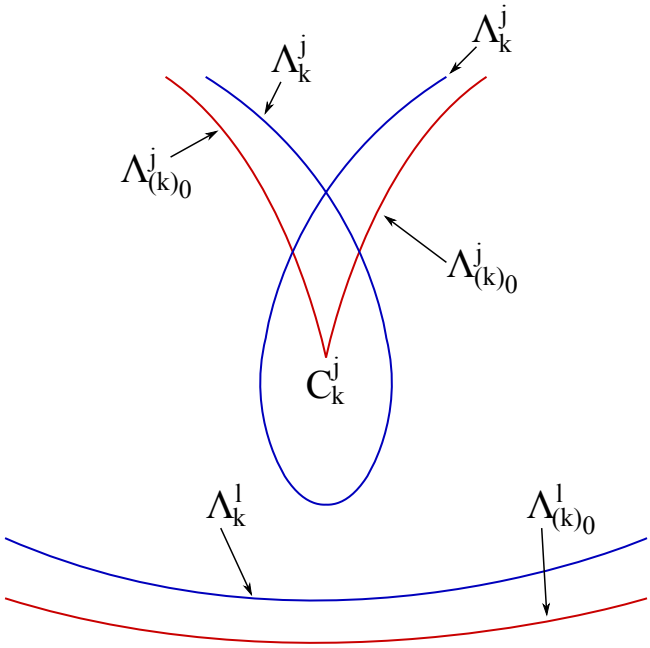

Figure 2.3 Parameter plane representation of a spring area related to a cusp point C^j_k and involving cycles of order k.

2.1.4.2 Synchronization

On n-dimensional coupled system, we define synchronization between subsystems as that the difference between state values of the subsystems is equal to 0, namely $x_p = x_q (p = 1, 2, 3, ..., n)(q \neq p)$.

2.1.5 Classical Properties of The 1-D Logistic Map

The logistic map is a polynomial mapping of degree 2, often cited as an archetypal example of how complex, chaotic behavior can arise from very simple nonlinear dynamical equations. The map was proposed as a discrete-time demographic model analogous to the logistic equation by the biologist Robert May The logistic map is written as

$$x_{n+1} = \alpha x_n (1 - x_n), \tag{2.8}$$

where, x_n is a number between zero and one, and represents the ratio of existing population at year n, and hence x_0 represents the initial ratio of population; and α is a positive number, and represents a combined rate for reproduction and starvation.

By varying the parameter α, the following behavior is observed. When $\alpha \in [0, 1]$, the population quickly converge to 0. When $\alpha \in (1, 2]$, the population quickly converge to the

value $1-(1/\alpha)$. When $\alpha \in (2,3]$, the population converge to the same value $1-(1/\alpha)$ with fluctuation. When $\alpha \in (3, 3.57)$, the population converge to permanent oscillations whose period is power-of-two. With α increasing, the period of oscillations increase from 2, then 4, 8, etc. This behavior is an example of a period-doubling cascade. When $\alpha \in (3, 3.57)$, Most parts of α exhibit chaotic behavior, but there are still certain isolated ranges of α that show non-chaotic behavior; these are called periodic window.

Figure 2.4 shows a bifurcation diagram which represents the cascade explained in the above. The bifurcation diagram is a fractal: if you zoom in on the value $\alpha = 3.82$ and focus on one arm of the three, the situation nearby looks like a shrunk and slightly distorted version of the whole diagram. The same is true for all other non-chaotic points. This is an example of the deep and ubiquitous connection between chaos and fractals.

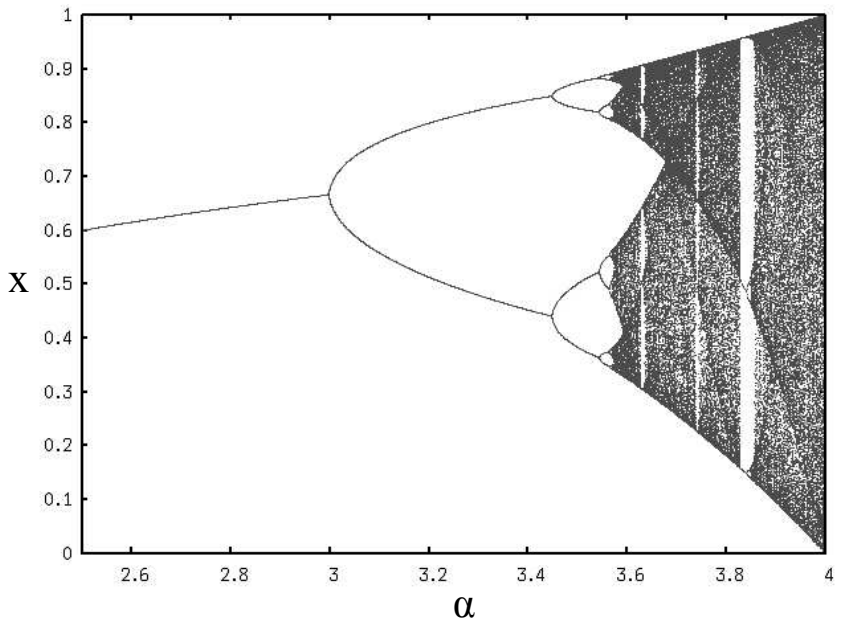

Figure 2.4 A bifurcation diagram of the logistic map.

The relative simplicity of the logistic map makes it an excellent point of entry into a consideration of the concept of chaos. A rough description of chaos is that chaotic systems exhibit a great sensitivity to initial conditionsa property of the logistic map for most values of α between about 3.57 and 4. A common source of such sensitivity to initial conditions is that the map represents a repeated folding and stretching of the space on which it is defined. In the case of the logistic map, the quadratic difference equation (2.8) describing it may be thought of as a stretching-and-folding operation on the interval $(0, 1)$.

Figure 2.6 illustrates the stretching and folding over a sequence of iterates of the map. The figure gives a two-dimensional phase diagram of the logistic map for $\alpha = 4$, and clearly shows the quadratic curve of the difference equation (2.8). Figure 2.5 demonstrates how initially nearby points begin to diverge. In the figure, two different but near points are set as the initial points x_0. These points suddenly draw apart and finally follow different trajectories.

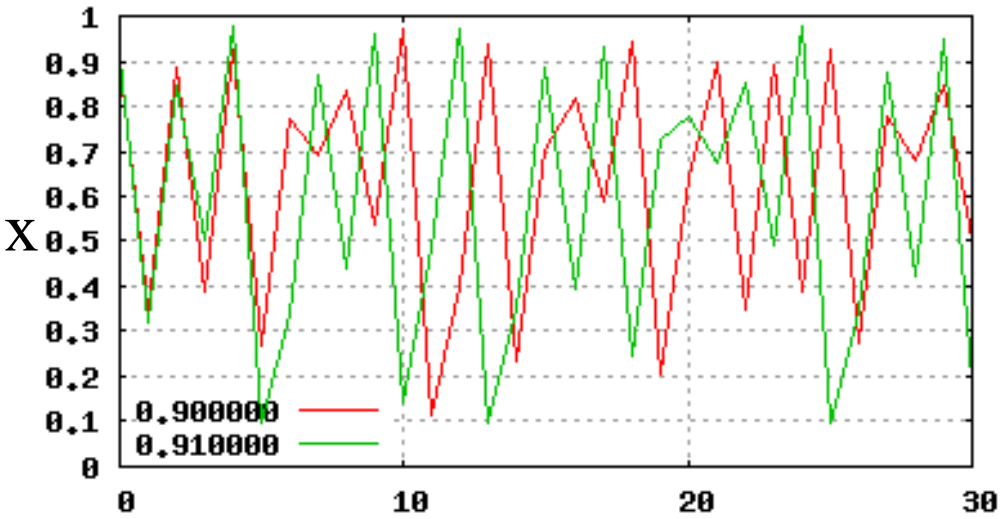

Figure 2.5 Time series of the logistic map.

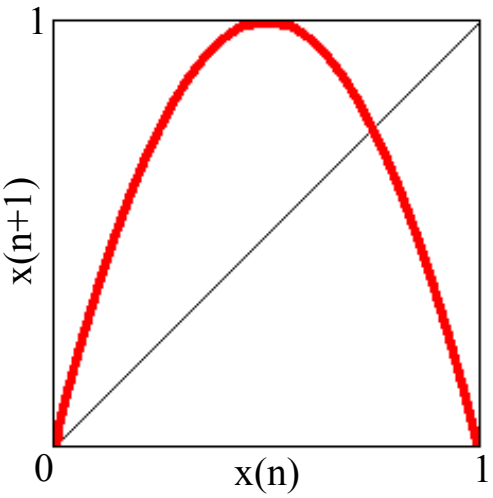

Figure 2.6 A return map of the logistic map for $\alpha = 4.0$.

2.2 Continuous-Time System

2.2.1 Poincaré Map

In mathematics, particularly in dynamical systems, a first recurrence map or Poincar map, named after Henri Poincar, is the intersection of a periodic orbit in the state space of a continuous dynamical system with a certain lower dimensional subspace, called the Poincar section, transversal to the flow of the system. More precisely, one considers a periodic orbit with initial conditions within a section of the space, which leaves that section afterwards, and observes the point at which this orbit first returns to the section. One then creates a map to send the first point to the second, hence the name first recurrence map. The transversality of the Poincar section means that periodic orbits starting on the subspace flow through it and not parallel to it. A Poincar map can be interpreted as a discrete dynamical system with a state space that is one dimension smaller than the original continuous dynamical system. Because it preserves many properties of periodic and quasi-periodic orbits of the original system and has a lower dimensional state space it is often used for analyzing the original system. In practice this is not always possible as there is no general method to construct a Poincar map. A Poincar map differs from a recurrence plot in that space, not time, determines when to plot a point. For instance, the locus of the moon when the earth is at perihelion is a recurrence plot; the locus

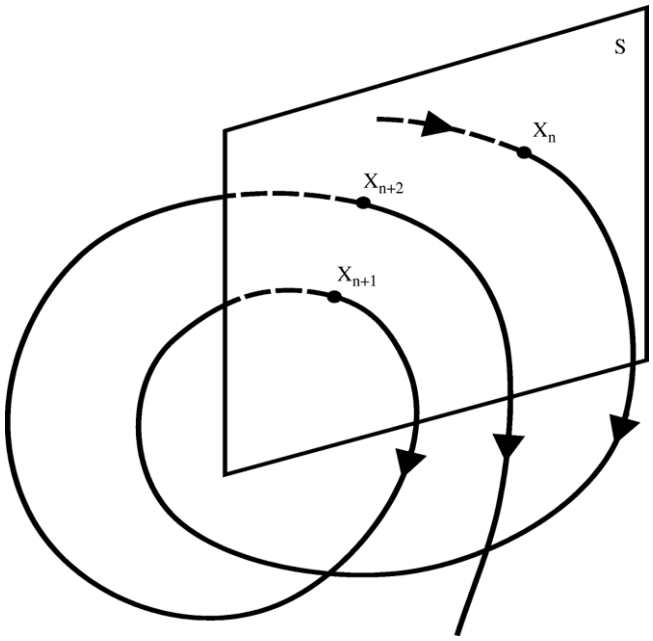

Figure 2.7 Poincaré map.

of the moon when it passes through the plane perpendicular to the Earth's orbit and passing through the sun and the earth at perihelion is a Poincar map. It was used by Michel H始on to study the motion of stars in a galaxy, because the path of a star projected onto a plane looks like a tangled mess, while the Poincar map shows the structure more clearly.

Consider an n-dimensional deterministic dynamical system.

$$\dot{x} = f(x), \tag{2.9}$$

and let S be an $n-1$ dimensional surface of section that is traverse to the flow, i.e., all trajectories starting from S flow through it and are not parallel to it. Then a Poincaré map P is a mapping from S to the next. Poincaré maps are useful when studying swirling flows near periodic solutions in dynamical systems.

2.2.2 Bifurcation

A local bifurcation occurs when a parameter change causes the stability of an equilibrium to change. In continuous systems, this corresponds to the real part of an eigenvalue of an equilibrium passing through zero. The equilibrium is non-hyperbolic at the bifurcation point. The topological changes in the phase portrait of the system can be confined to arbitrarily small neighbourhoods of the bifurcating fixed points by moving the bifurcation parameter close to the bifurcation point. More technically, consider the continuous dynamical system described by the ordinary differential equation

$$\dot{x} = f(x, \lambda) \qquad f : R \times R \to R. \tag{2.10}$$

A local bifurcation occurs at $(x_0, z\lambda_0)$ if the Jacobian matrix $df_{x0,\lambda 0}$ has an eigenvalue with zero real part. If the eigenvalue is equal to zero, the bifurcation is a steady state bifurcation, but if the eigenvalue is non-zero but purely imaginary, this is a Hopf bifurcation.

2.2.3 Classical Properties of Chua's Circuit

Chua's circuit (Fig. 2.8) is a nonlinear electronic circuit that is the object of much scientific research activities. This circuit contains four linear elements (two capacitors, one inductor, and one resistor) and a nonlinear resistor, called Chua's diode, which can be built using off-the-shelf Op-Amps. Since Chua's circuit is endowed with an unusually rich repertoire of nonlinear dynamical phenomena, it has become a universal paradigm for chaos.

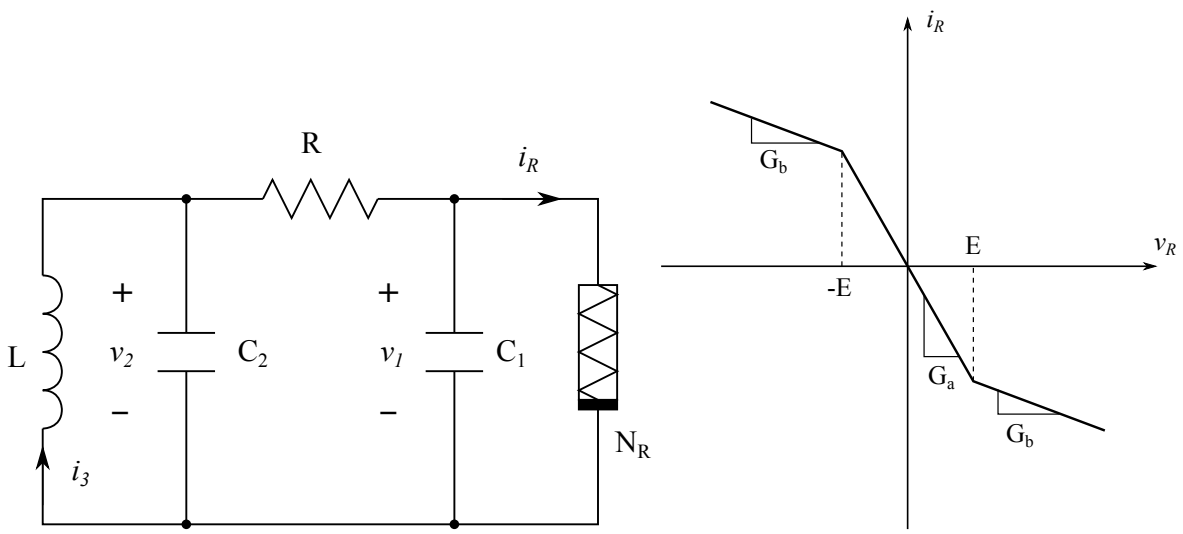

Figure 2.8 The circuit model of Chua's circuit and the $i-v$ characteristics of the nonlinear resistor N_R.

The state equations of Chua's circuit are:

$$\begin{cases} \dfrac{dv_1}{dt} = \dfrac{1}{C_1}\left\{\dfrac{1}{R}(v_2 - v_1) - f(v_1)\right\} \\ \dfrac{dv_2}{dt} = \dfrac{1}{C_2}\left\{\dfrac{1}{R}(v_1 - v_2) + i_3\right\} \\ \dfrac{di_3}{dt} = -\dfrac{1}{L}v_2 \end{cases}, \tag{2.11}$$

and

$$f(v_1) = G_b v_1 + \frac{1}{2}(G_a - G_b)\{|v_1 + E| - |v_1 - E|\} \tag{2.12}$$

is the $v - i$ characteristic of the nonlinear resistor N_R with a slope equal to G_a in the inner region and G_b in the outer region. A typical $v - i$ characteristic of N_R is shown in Fig. 2.8(b). By using following parameters and variables:

$$\begin{cases} \tau = \dfrac{1}{RC_2}t, \alpha = \dfrac{C_2}{C_1}, \beta = \dfrac{R^2 C_2}{L} \\ x = \dfrac{v_1}{E}, y = \dfrac{v_2}{E}, z = \dfrac{R}{E}i_3, \end{cases} \tag{2.13}$$

the normalized circuit equations are given as:

$$\begin{cases} \dfrac{dx}{d\tau} = \alpha \{y - x - f(x)\} \\ \dfrac{dy}{d\tau} = x - y + z \\ \dfrac{dz}{d\tau} = -\beta y \end{cases} . \tag{2.14}$$

In Chua's circuit, when the resistance R is varied, a bifurcation route to chaos represented as the following is observed. Figure 2.10 shows an one-parameter bifurcation diagram to chaos with decreasing of resistance R. In this route to chaos, an equilibrium point loses stability and a stable limit cycle emerges through an Andronov-Hopf bifurcation when the resistance R is decreased. As the value of R is further decreased, the stable limit cycle eventually loses stability, and a stable limit cycle of approximately twice the period emerges, which we shall refer to as as period-2 limit cycle. As R is decreased further, this period-2 limit cycle in turn loses stability, and a stable period-4 limit cycle appears. This bifurcation occurs infinitely many times at ever-decreasing intervals of resistance parameter range which converges at a geometric rate to a limit (bifurcation point) at which point chaos is observed. This is illustrated in Fig. 2.10(a)-(e),

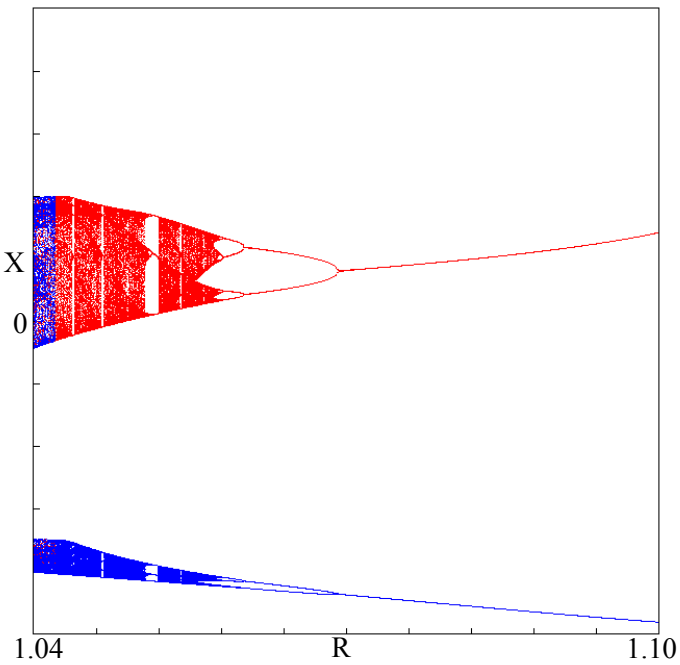

Figure 2.9 An example of one-parameter bifurcation diagram in Chua's circuit.

where we start with a stable limit cycle (Fig. 2.10(a)), and followed by a stable period-2 limit cycle (Fig. 2.10(b)), a stable period-4 limit cycle (Fig. 2.10(c)), a stable period-8 limit cycle (Fig. 2.10(d)) and finally a spiral Chua's attractor (Fig. 2.10(e)).

After the appearance of chaos on the route with decreasing of R, some parameter regions where periodic limit cycles emerge are observed. A stable period-3 limit cycle (Fig. 2.10(f)) is observed between the parameter regions where chaotic attractors are observed. In parameter regions presented above, two symmetric attractors centered unstable equilibrium points which are symmetrically located at the origin coexist. As R is decreased further, two coexisting attractors merge into a chaotic attractor spreading over both of positive and negative regions (Fig. 2.10(h)). The chaotic attractor is called a double-scroll attractor.

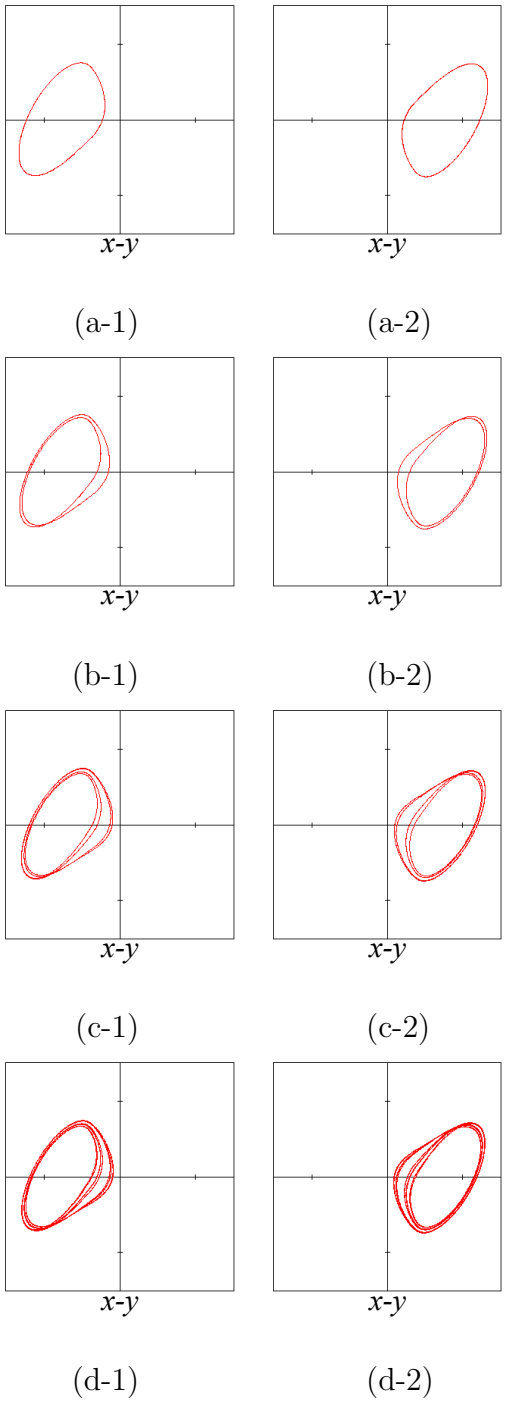

Figure 2.10 Attractors in Chua's circuit. (a)-(g)Two coexisting attractors for several periods or chaos. (h) A double scroll attractor.

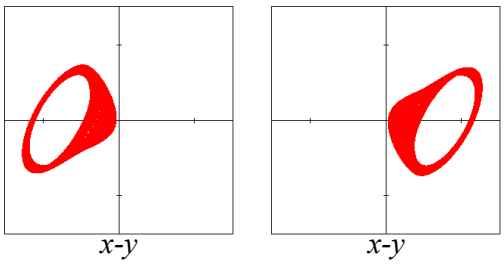

(e-1) (e-2)

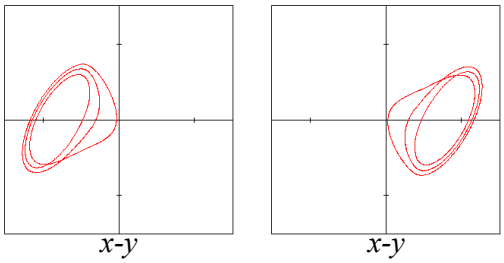

(f-1) (f-2)

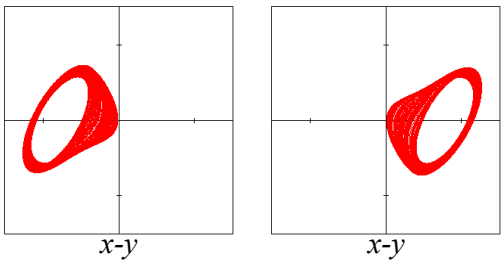

(g-1) (g-2)

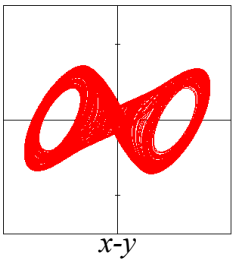

(h)

Figure 2.10 *Continued.*

Chapter 3

Parametrically Forced Discrete-Time System

3.1 Introduction

In this chapter, we firstly introduce N-dimensional globally coupled system involving periodic parametric force and and general properties of the system. The properties are caused by the periodic parameter force. Then, we investigate one or two dimensional case of the parametrically forced system when the logistic map is used for the one-dimensional subsystem constructing the parametrically forced system, and demonstrate the properties of the system.

3.2 N-dimensional Coupled Parametrically Forded Discrete-Time System

The N-dimensional parametrically forced system is constructed of the coupling with mutually influencing scheme of identical one-dimensional subsystems whose parameters are forced into periodic varying. The system is described as:

$$T : \begin{cases} x_p(n+1) = (1-\varepsilon)F(x_p(n), \alpha_f(n)) \\ \qquad\qquad + \dfrac{\varepsilon}{N}\displaystyle\sum_{j=1}^{N} F(x_j(n), \alpha_f(n)) \qquad , \\ \qquad\qquad (p = 1, .., N) \quad (n = 0, 1, 2, ...) \end{cases} \tag{3.1}$$

and

$$\alpha_f(n) = \begin{cases} \alpha_1, & \text{for each odd value of “}n\text{”} \\ \alpha_2, & \text{for each even value of “}n\text{”} \\ & (n = 0, 1, 2, ...) \end{cases} . \tag{3.2}$$

The parameter α_f alternately changes from α_1 to α_2 and $\varepsilon \in [0, 1]$. This system is not continuous in iteration because α_f is periodically changed. Nevertheless, the twice iteration of this

system is continuous because of the order 2 of the periodicity regarding α_f.

3.3 General properties of maps T

We firstly characterize some general properties of the N-dimensional parametrically forced system. We define T_o as the mapping from odd number iteration, while T_e is the mapping from even number iteration,

$$\begin{aligned} X(2n+2) &= T_o(X(2n+1)) = T(X_{2n+1}, \alpha_1) \\ X(2n+1) &= T_e(X(2n)) = T(X_{2n}, \alpha_2) \\ & \qquad (n = 0, 1, 2, ...) \end{aligned} \quad , \tag{3.3}$$

and let

$$\begin{aligned} T^2_{odd}(X) &= T_e \circ T_o(X) \\ T^2_{even}(X) &= T_o \circ T_e(X) \end{aligned} \quad . \tag{3.4}$$

Then the trajectories are obtained such as follows, if the number of iteration n is even,

$$X(n) = T_o \circ T_e \circ T_o \circ \cdots \circ T_o \circ T_e(X_0), \tag{3.5}$$

and if the number of iteration n is odd,

$$X(n) = T_e \circ T_o \circ T_e \circ \cdots \circ T_o \circ T_e(X_0). \tag{3.6}$$

From these things, the following relations are obtained.

$$\begin{aligned} T_o \circ T^{2n}_{odd}(X) &= T^{2n}_{even} \circ T_o(X) \\ T_e \circ T^{2n}_{even}(X) &= T^{2n}_{odd} \circ T_e(X) \end{aligned} \quad . \tag{3.7}$$

Theorem 1. *A necessary condition for fixed point of T is:*

$$T_o(X) = T_e(X) = X. \tag{3.8}$$

Proof . Assuming X is a fixed point obtained from only T_o and X' is a fixed point obtained from T_e.

$$\begin{aligned} T_o(X) &= X \\ T_e(X') &= X'. \end{aligned} \tag{3.9}$$

If X' is not a fixed point of T_o, mapping from X' with T_o cannot give X'. While, mapping from X with T_e cannot give X if X is not a fixed point of T_e.

$$\begin{aligned} T_o(X') &\neq X' \\ T_e(X) &\neq X. \end{aligned} \tag{3.10}$$

Then,

$$\begin{aligned} T_e \circ T_o(X) &\neq X \\ T_o \circ T_e(X') &\neq X'. \end{aligned} \tag{3.11}$$

Therefore, the necessary condition of fixed point of T is:

$$T_o(X) = T_e(X) = X. \tag{3.12}$$

Theorem 2. *If an orbit $(X_0, X_1, ..., X_{k-1})$ is an odd order k cycle,*

$$T_e(X_i) = T_o(X_i), \quad i = 0, 1, 2, ..., k-1 \tag{3.13}$$

Proof . Let be $X_0, X_1, X_2, \cdots X_{k-1}$ an odd order k cycle of T, then, each mapping from X_1 to X_{2k} is obtained as follows.

$$\begin{aligned} T_e(X_0) &= X_1 \\ T_o(X_1) &= X_2 \\ T_e(X_2) &= X_3 \\ &\vdots \\ T_e(X_{k-1}) &= X_k = X_0 \\ T_o(X_k) &= T_o(X_0) = X_1 \\ T_e(X_{k+1}) &= T_e(X_1) = X_2 \\ &\vdots \\ T_e(X_{2k}) &= T_e(X_k) = X_1. \end{aligned} \tag{3.14}$$

From this, the following relationship is obtained.

$$T_e(X_i) = T_o(X_i), \quad i = 0, 1, 2, ..., k-1 \tag{3.15}$$

This property is always true for points of even-order cycles.

These properties imply that generally odd-order cycles do not exist in this system. Indeed, T_e and T_o have different parameters, so generally $T_e(X_i)$ is not equal to $T_o(X_i)$ in the case of an odd order cycle. Moreover, these properties also imply that two same cyclic points can appear during one period of a cycle. As an example, we consider an order 6 cycle $(X_1, X_2, X_3, X_4, X_5, X_6)$. In this cycle, it is possible that X_1 is equal to X_4, while, each of the other cyclic points has a distinct value. The 6-cycle is a real 6-cycle and not a 3-cycle. Because it is possible that mappings from different coordinates with T_o and T_e give the same next coordinates, namely $T_o(X_3) = T_e(X_6) = X_4 = X_1$. Moreover, mappings from the same coordinates with T_o and T_e give different next coordinates, namely $T_o(X_1) \neq T_e(X_4)$. In this system, we observe interesting

behaviors due to the periodically parameter changing. We shall see in next section that these properties can imply that odd-order cycles do not exist.

3.4 Peculiar Case of The 1-D Logistic Map

In this study, we use logistic map as the one-dimensional subsystem in the parametrically forced system. The equation of the logistic map is:

$$X(n+1) = \alpha_f(n)X(n)(1 - X(n)) = F(X(n), \alpha_f(n)), \tag{3.16}$$

where, the parameter $\alpha_f(n)$ is forced into periodic varying (3.2).

In order to investigate evolution of bifurcations depending on the coupling, firstly, one-dimensional non-coupled case is considered. In the case of one-dimensional parametrically forced system, the equation of the system becomes the same as Eq. (3.16).

Figure 3.1 shows examples of a return map of the parametrically forced logistic map. For the original logistic map, two-periodic solution is observed for $\alpha = 3.0$, while, three-periodic solution is observed for $\alpha = 3.83$. These two solutions are periodic, whereas in the logistic map involving parametric force, a solution is chaotic as shown in Fig. 3.1(a) when the parameters α_1 and α_2 are set 3.0 and 3.83, respectively. Namely, chaotic solution can be observed in the combination of two parameters that generate two kinds of periodic solutions.

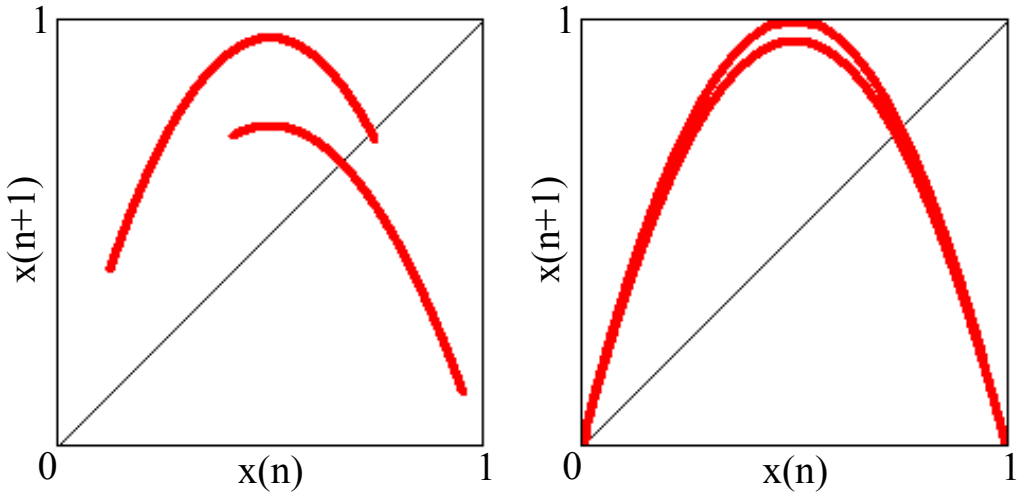

(a) (b)

Figure 3.1 Return maps of parametrically forced logistic map. (a) $\alpha_1 = 3.0$ and $\alpha_2 = 3.83$. (b) $\alpha_1 = 3.80$ and $\alpha_2 = 4.00$.

3.4.1 Bifrucations

Figure 3.2 shows a bifurcation diagram. Each colored domain indicates existence of at least one stable cycle whose order corresponds to upper colored squares in the figure. Only even-order cycles are observed except fixed point and the case of $\alpha_1 = \alpha_2$. This can be proved easily from the **Theorem 2** which gives the necessary condition of existence of odd-order cycles. In the parametrically forced logistic map, the parameter is forced and alternately changes from α_1 to α_2. $T_o(X, \alpha_1)$ and $T_e(X, \alpha_2)$ have different parameters if $\alpha_1 \neq \alpha_2$. Mappings from the same coordinate with T_o and T_e cannot give the same results. Therefore, odd-order cycles cannot exist in the parametrically forced logistic map, when $\alpha_1 \neq \alpha_2$.

Figure 3.3 shows bifurcation curves of order 2, 4 and 8 cycles. Bifurcation curves are ob-

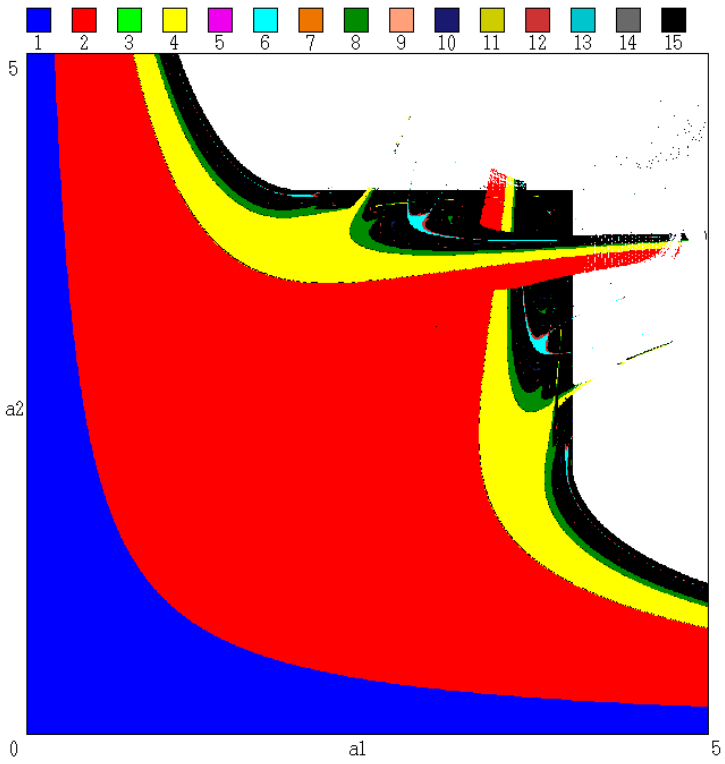

Figure 3.2 Representation of the parameter plane (α_1, α_2). Each colored part corresponds to the existence of a stable cycle (periodic point), the order k (period) of which is given by the upper colored squares. The black color corresponds to $k \geq 15$ or to chaos. The white region corresponds to the nonexistence of attracting set, with chaotic transient toward infinity. Horizontal axis: α_1. Vertical axis: α_2.

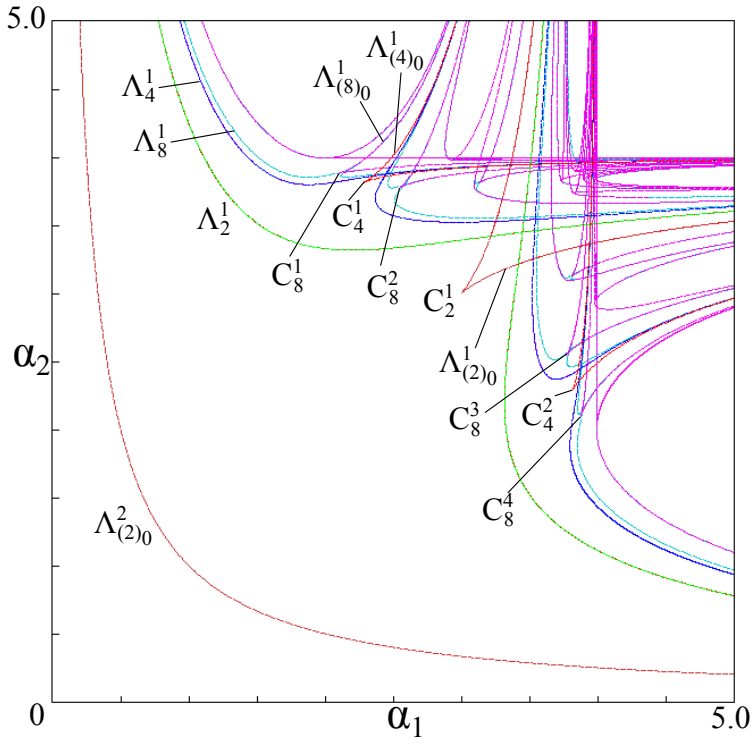

Figure 3.3 Bifurcation curves related to order 2, 4 and 8 cycles. Orange and green curves correspond to fold and flip bifurcations of order 2 cycles, respectively. Red and blue curves correspond to order 4 cycles, and purple and cyan curves correspond to order 8 cycles.

tained using analytical-numerical methods [29]. In the figure, a locus of bifurcation ($\partial F^k/\partial X = 1$ where F^k is the k^{th}-iteration by F) is a fold bifurcation curve denoted $\Lambda^j_{(k)_0}$ and a locus of bifurcation ($\partial F^k/\partial X = -1$) is a flip bifurcation curve denoted Λ^j_k. The index j is a number characterizing the considered order k cycle. Because of the order 2 of the periodicity, only bifurcation curves regarding even-order cycles can be obtained. However, this condition is sufficient to obtain all bifurcation curves because odd-order cycles do not exist in the system.

Also, bifurcation curves regarding order 2 cycles are obtained analytically and given by:

$$\begin{aligned} &\Lambda^{2}_{(2)_0} : \alpha_1\alpha_2 = 1 \\ &\Lambda^{1}_{(2)_0} : \alpha_1^2\alpha_2^2 - 4\alpha_1^2\alpha_2 - 4\alpha_1\alpha_2^2 + 18\alpha_1\alpha_2 - 27 = 0 \\ &\Lambda^{1}_{2}, \Lambda^{1'}_{2} : 12\alpha_1\alpha_2^2 - 4\alpha_1^2\alpha_2^3 + 15\alpha_1^2\alpha_2^2 - 85\alpha_1\alpha_2 + \alpha_1^3\alpha_2^3 \\ &\qquad -4\alpha_1^3\alpha_2^2 + 12\alpha_1^2\alpha_2^2 + 12\alpha_1^2\alpha_2 + 125 = 0 \end{aligned} \quad . \tag{3.17}$$

The bifurcation curves well correspond to the boundaries between colored domains in Fig. 3.2. The bifurcation structure is symmetric with regard to the diagonal ($\alpha_1 = \alpha_2$). On the parameter plane, crossroad areas (in the sense of [23]) centered at fold cusp points regarding to several orders can be detected.

Figure 3.4 shows a one-parameter bifurcation diagram when α_1 is fixed at 3.84 and α_2 varies. The fixed point $x = 0$ undergoes the bifurcation point $\alpha_1 = 1/\alpha_2$ and then an order 2 cycle

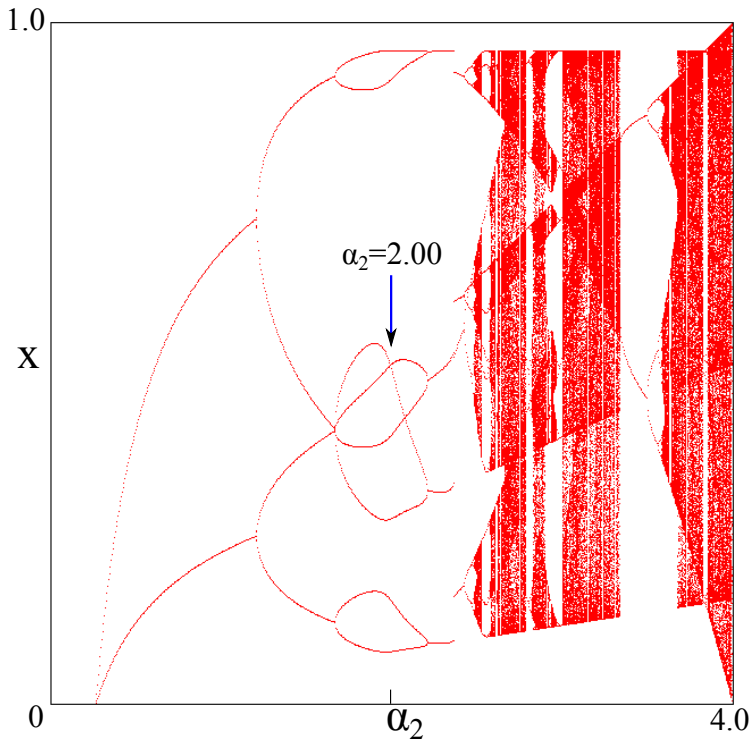

Figure 3.4 An example of one-parameter bifurcation diagram whose parameter α_1 is fixed at 3.84.

appears. After that, the cycle continues to undergo bifurcations and the bifurcation cascade gives rise to chaos. At the point where curves of periodic cycle cross to others such as $\alpha_2 = 2.00$ in the figure, a coordinate appears twice in a cycle. When $\alpha_2 = 2.00$, the coordinate $X = 0.50$ appears twice in the order 8 cycle.

As seen above, interesting behaviors which are caused by the periodically parameter changing such nonexistence of odd-order cycles and twice-appearance of a coordinate in a cycle are observed. We shall see that these behaviors can be observed in the system for any dimensional case.

3.5 Peculiar Case of The 2-D Logistic Map

In this section, we consider the two-dimensional case, two parametrically forced logistic maps are coupled with the mutually influencing scheme.

$$T : \begin{cases} x(n+1) = (1-\frac{\varepsilon}{2})F(x(n), \alpha_f(n)) + \frac{\varepsilon}{2}F(y(n), \alpha_f(n)) \\ y(n+1) = (1-\frac{\varepsilon}{2})F(y(n), \alpha_f(n)) + \frac{\varepsilon}{2}F(x(n), \alpha_f(n)) \\ \qquad\qquad\qquad\qquad\qquad\qquad (n = 0, 1, 2, ...) \end{cases} . \tag{3.18}$$

We investigate behaviors on parameter plan and phase plane in the two-dimensional system.

3.5.1 Bifurcation

In this subsection, bifurcations are investigated with respect to α_f. Figure 3.5 shows a two-parameter bifurcation diagram and its enlargement when ε is fixed at 0.04 and α_1 and α_2 are changed. In the parameter (α_1, α_2) plane, the existence domain of attracting set at finite distance is given by the colored part of Fig. 3.5. Only even periodic orbits are observed except fixed point and the case of $\alpha_1 = \alpha_2$. In the figure, some discontinuous boundaries of bifurcation are observed, for instance smooth boundary between green region and black region is intercepted by protuberant green region in Fig. 3.5(b). This discontinuity is caused due to multistability and initial conditions of calculation. In some regions, multistability behaviors can be observed. Different attractors can coexist, depending on the choice of different initial conditions. An example of the coexistence is shown in Fig. 3.6 when $\alpha_1 = 2.94$, $\alpha_2 = 3.84$ and $\varepsilon = 0.04$. In this figure, period 6 orbit and chaotic orbit coexist, these orbits correspond to different initial values of (x_1, x_2).

In the next section, basin which is an initial value set converging to a given orbit is investigated for parameter values corresponding to multistability.

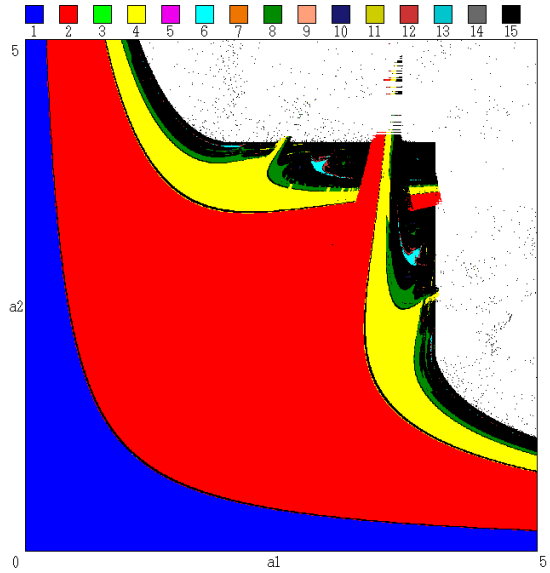

(a)

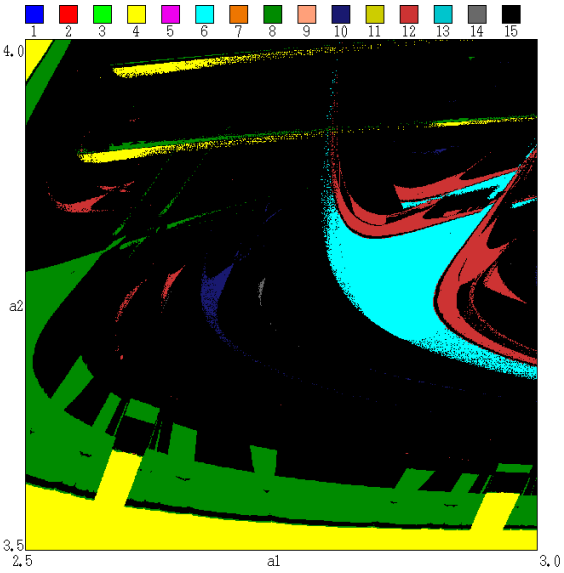

(b)

Figure 3.5 Representation of the parameter plane (α_1, α_2). Each colored part corresponds to the existence of a stable cycle (periodic point), the order k (period) of which is given by the upper colored squares. The black color corresponds to $k \geq 15$ or to chaotic behavior. The white region corresponds to the nonexistence of attracting set, with chaotic transient toward infinity. Horizontal axis: α_1. Vertical axis: α_2. (b) Enlargement of (a)

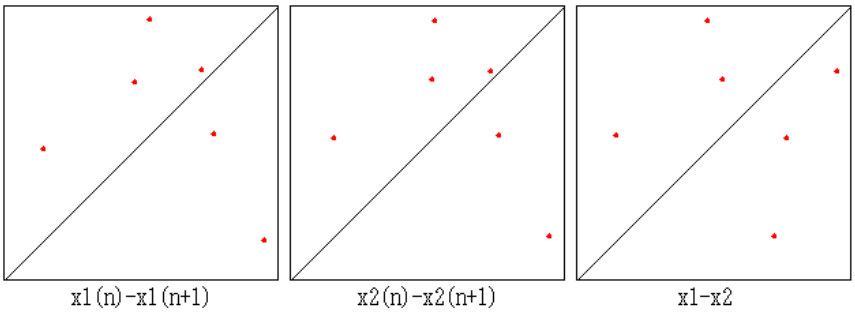

(a)

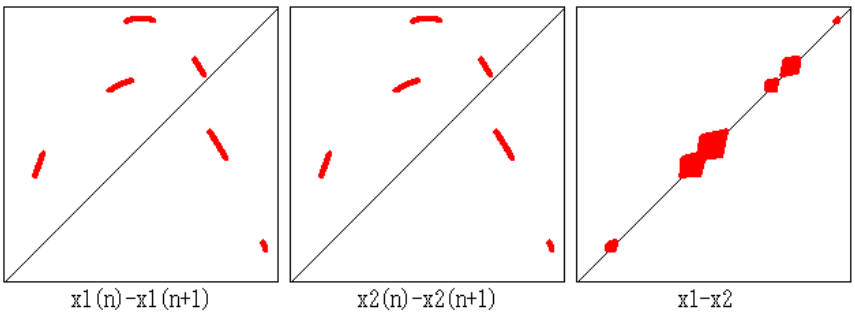

(b)

Figure 3.6 return maps and phase differences in coexistence of period six orbit and chaotic orbit depending on initial values. $\alpha_1 = 2.94$, $\alpha_2 = 3.84$ and $\varepsilon = 0.04$.

3.5.2 Basin

Depending on the property of the system, α_f is changed every update periodically. Figure 5.4 shows basin when the parameters α_2 and ε are considered as having fixed values, α_1 varies with increasing values. Each basin of attraction, represented by a different color, corresponds to the period of orbit. Basins in Fig. 5.4(a) consist of the region having period 6 orbit, represented by cyan, and the region having chaotic orbit, represented by black. Increasing α_1, basins are changing because there is coexistence of a period 12 orbit and a chaotic orbit. More increasing α_1, we obtain three kinds of orbits, which are period 6 orbit, period 12 orbit and chaotic orbit.

In the basins, fractal structures are confirmed at the corner of each basin. Figures 3.8 show the enlargement around a corner of basin in Fig. 5.4(a) and its enlargements. With repeating enlargement, similar structure continues.

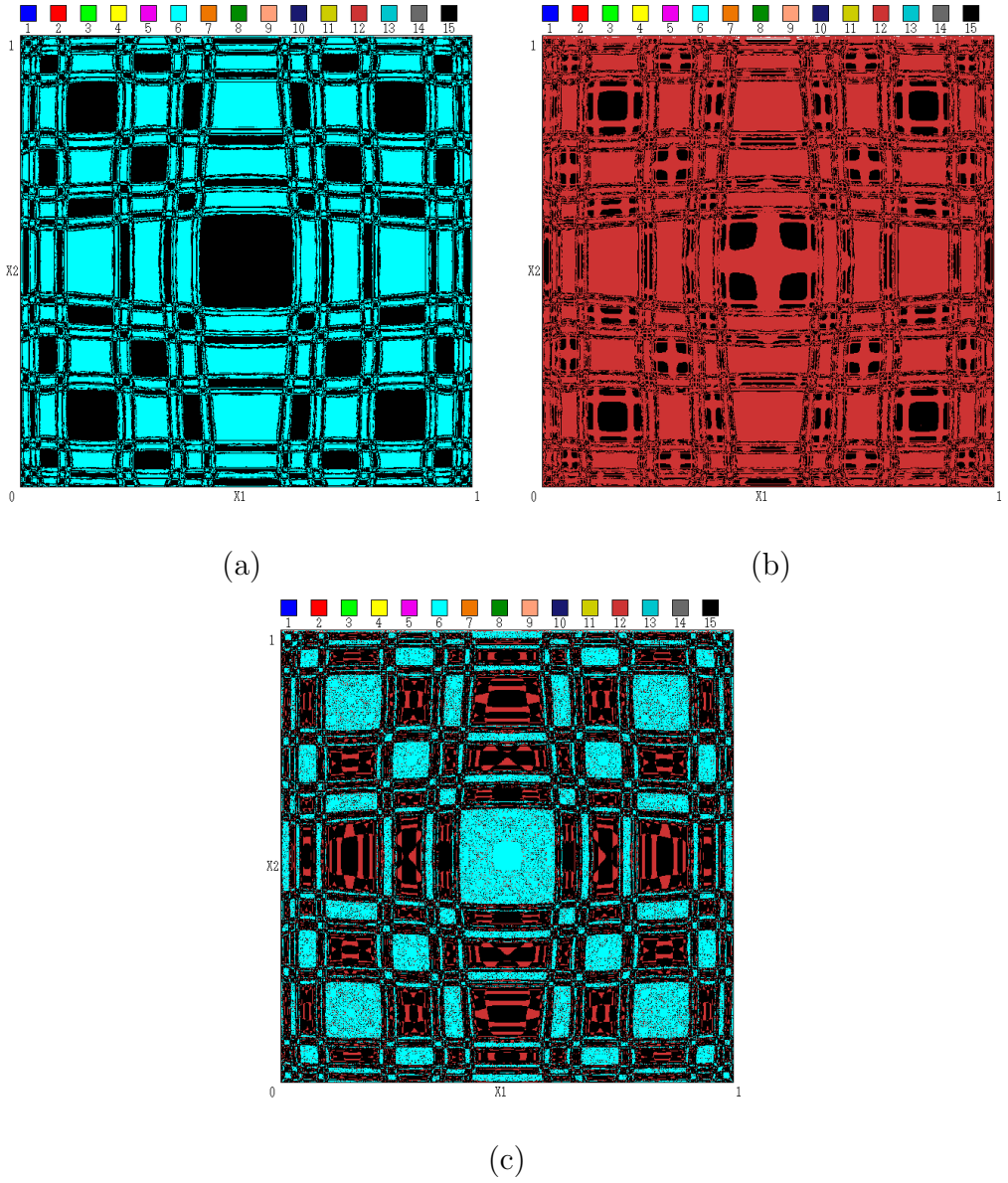

Figure 3.7 Basin regarding to T for $\alpha_2 = 3.84$ and $\varepsilon = 0.04$. (a) $\alpha_1 = 2.94$. (b) $\alpha_1 = 2.97$. (c) $\alpha_1 = 2.98$. Horizontal axis: x_1. Vertical axis: x_2.

3.5.3 Periodic orbits

The parametrically forced logistic map is not continuous in iteration because α_f is periodically changed. Then, in order to obtain periodic orbits of T, that are all even, we consider T^2. An order k periodic orbit of T^2 will be an order $2k$ periodic orbit of T. So we will obtain all even periodic orbits of T by calculating all periodic orbits of T^2. All order k periodic orbits of T^2 will be obtained by considering T^2_{even} and T^2_{odd} and by applying Newton method to the

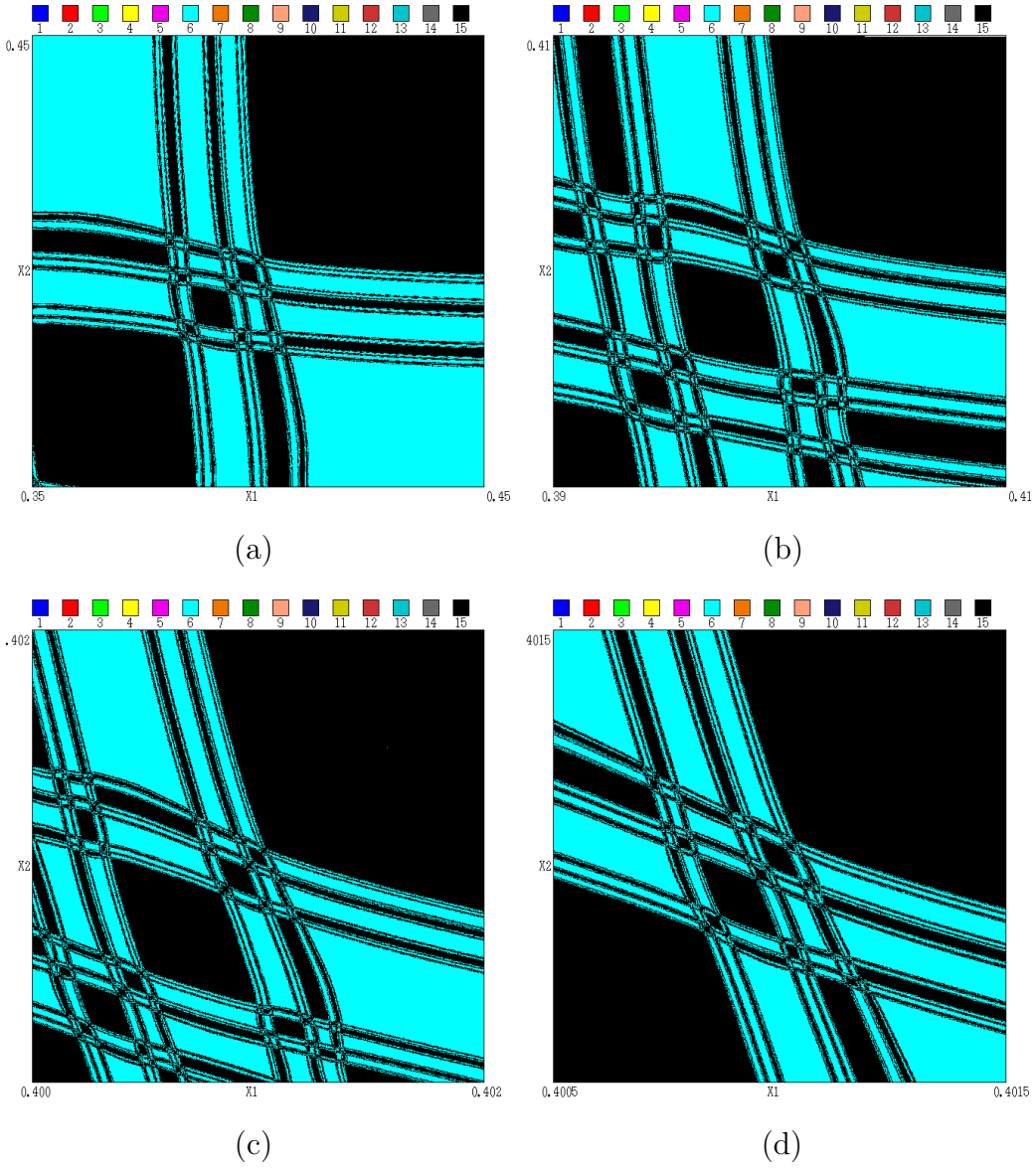

Figure 3.8 Enlargement around a corner of basin. $\alpha_1 = 2.94$, $\alpha_2 = 3.84$ and $\varepsilon = 0.04$. (a) Enlargement in [0.3, 0.4]. (b) Enlargement in [0.35, 0.38]. (c) Enlargement in [0.369, 0.365]. (d) Enlargement in [0.3615, 0.3625]. Fractal structures are shown.

equations $T^2_{even}(X) = X$ and $T^2_{odd}(X) = X$. T^2_{even} and T^2_{odd} are differentiable. Thus, Newton method can be applied. In Figure 3.9, dots indicate order 3 periodic orbits of T^2 which are detected by superimposing the order 3 periodic orbits calculated on T^2_{even} and T^2_{odd}. Purple dots correspond to stable order 3 periodic orbit of T^2, red points correspond to saddle, and yellow dots correspond to unstable node. Saddles are plotted on the corner of boundaries between

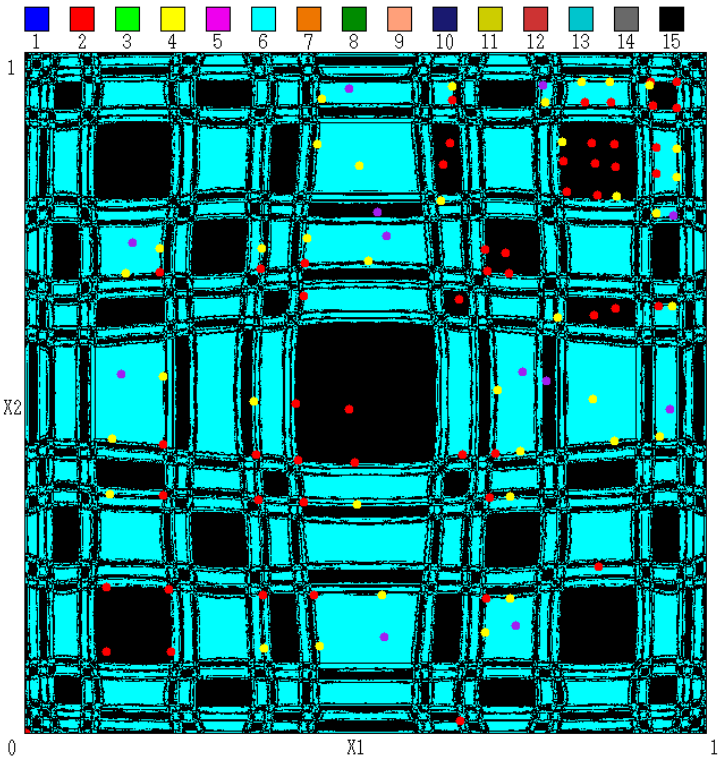

Figure 3.9 Order 3 periodic orbits of T^2. $\alpha_1 = 2.94$, $\alpha_2 = 3.84$ and $\varepsilon = 0.04$. Purple dots correspond to stable order 3 periodic orbit of T^2, red points correspond to saddle, and yellow dots correspond to unstable node.

basins. Then, it appears that stable manifold of saddle is a part of boundaries of basins.

3.6 Conclusion

In this chapter, we introduced N-dimensional coupled system whose parameter is forced into periodic varying, the system been constructed of n one-dimensional subsystems with globally coupling scheme. We detected general properties for the system. The properties are obtained from the periodic varying of the parameter and implicit non-existence of odd order cycles in the system.

Then, one-dimensional non-coupled case was considered. We investigated one-dimensional case of the parametrically forced system when the logistic map is used for the one-dimensional subsystem constructing the parametrically forced system. Only even-order cycles are observed except fixed point and the case of $\alpha_1 = \alpha_2$. On the parameter plane, crossroad areas centered at fold cusp points regarding to several orders are detected. The properties of the system are

demonstrated in the investigation when the logistic map is used for the one-dimensional subsystem constructing the parametrically forced system in one-dimensional case. The properties are common in any-dimensional case.

Finally, two-dimensional case was considered. From the investigations of bifurcation, we confirmed that all the orbits correspond to only even order cycles except fixed point and the special case that α_1 equals to α_2. Moreover, existence of coexisting attractors, which consist of cycle orbit or chaotic orbit, is confirmed. Then, basin has been investigated when the coexistence occurs. In the basins, fractal structure appears. Periodic orbits and their basins are numerically calculated by using second order iteration and superposition with Newton method. By calculating its eigenvalues, it was confirmed that saddles are on the corner of boundaries between basins.

Chapter 4

Parametrically Forced Chua's Circuit with Identical Forces

4.1 Introduction

In this chapter, we propose a coupled Chua's circuit whose parameter is forced into periodic varying in associated with the period of an internal state value of one of the coupled subcircuits and investigate behaviors by carrying out computer simulations and circuit experiments. Since, forces given to all subcircuits are controled by one of the subcircuits, the controlling subcircuit and the remain subcircuits are assumed to be master-slave relationship. In the next section, we propose the coupled parametrically forced Chua's circuit. In section 3, we investigate bifurcations in the non-coupled parametrically forced Chua's circuit by carrying out computer simulations and circuit experiments. Non-existence of odd order cycles and coexistence of different attractors are observed. In section 4, we investigate synchronizations in the coupled parametrically forced Chua's circuit. Coexisting of many attractors whose synchronizations states are different are observed. In section 5, observed phenomena in the system is compared with a parametrically forced discrete-time system. Similar phenomena are confirmed between the parametrically forced discrete-time system and the parametrically forced Chua's circuit. The last section is devoted to the conclusion.

4.2 Parametrically forced Chua's circuit

We consider a coupled continuous-time system whose parameter is forced into periodic varying. Chua's circuit is used as the continuous-time system. Subcircuits in the parametrically forced Chua's circuits are coupled with the all other subcircuits via resistors. The circuit model of the coupled system is shown in Fig. 5.1. For this coupling, $v_{1k}(k = 1, 2)$ affect to the other subcircuits with the coupling intensity corresponding to the coupling resistor. The linear

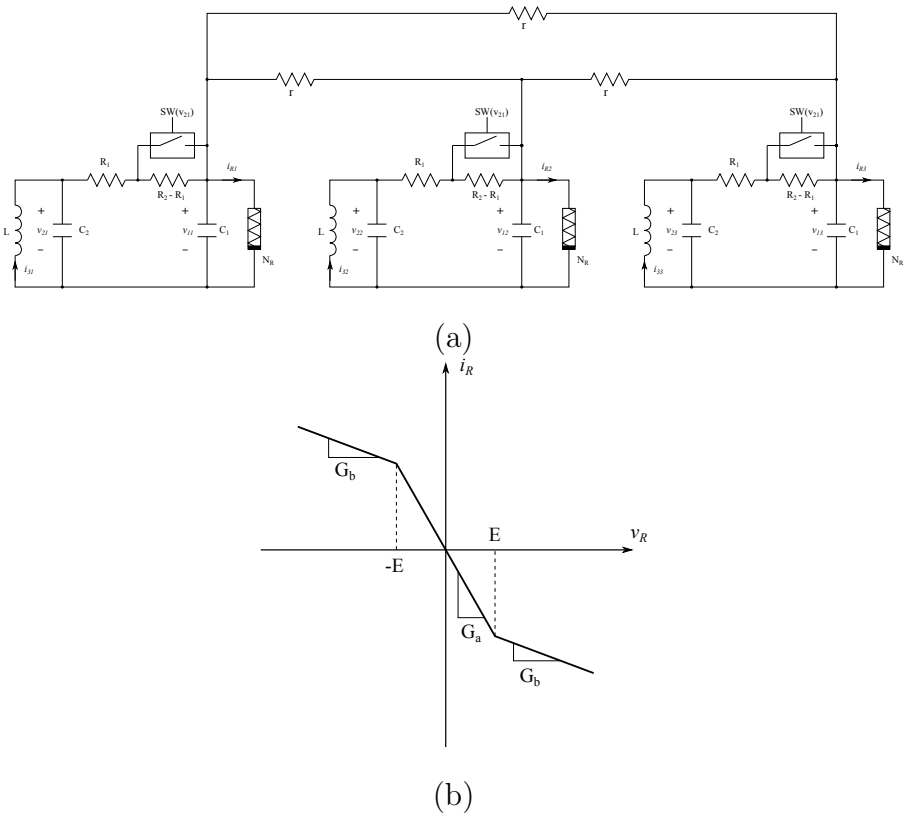

Figure 4.1 The circuit model of the parametrically forced Chua's circuit and the $i - v$ characteristics of the nonlinear resistor N_R.

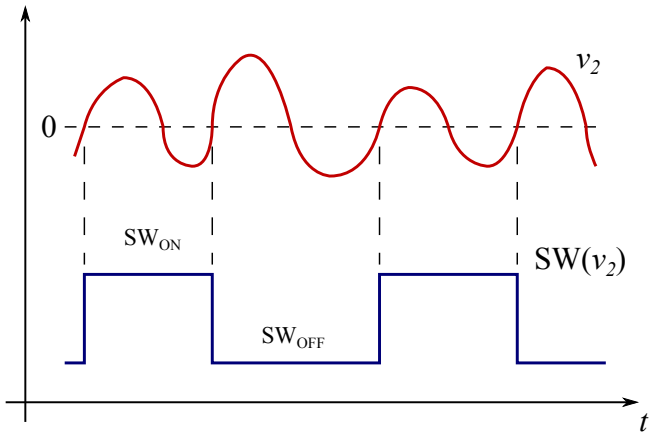

Figure 4.2 The motion of the switch depending on v_2.

resistors of the Chua's circuits alternately changes from R_1 to R_2 depending on v_{21}. The switches which cause periodic varying of the resistors are controlled by v_{21}. Namely, the switches are controlled by the state value of one of the subcircuit. The switches shift when v_{21} is equal to 0 and changes from negative value to positive value. Figure 5.2 shows the relationship between

v_{21} and the motion of the switch. The linear resistor are changed every one period of v_{21}. For circuit implementation of the switches, the control system of the switch is composed of a detection circuit of the rise time of v_{21} and a system that state value has two values and shifts from one value to the other value depending on the rise time. We realize the control system of the switch by using OP amps and flip-flop circuits.

The state equations of the parametrically forced Chua's circuit are:

$$\begin{cases} \dfrac{dv_{1k}}{dt} = \dfrac{1}{C_1}\left\{\dfrac{1}{R}(v_{2k} - v_{1k}) - f(v_{1k}) + \dfrac{1}{r}(\sum_{i=1}^{N} v_{1i} - Nv_{1k})\right\} \\ \dfrac{dv_{2k}}{dt} = \dfrac{1}{C_2}\left\{\dfrac{1}{R}(v_{1k} - v_{2k}) + i_{3k}\right\} \\ \dfrac{di_{3k}}{dt} = -\dfrac{1}{L}v_{2k} \\ (k = 1, 2, ..., k) \end{cases}, \tag{4.1}$$

where, N is the number of coupled subcircuits and R alternately changes from R_1 to R_2 depending on v_{21}; and

$$f(v_{1k}) = G_b v_{1k} + \frac{1}{2}(G_a - G_b)\{|v_{1k+}E| - |v_{1k} - E|\} \tag{4.2}$$

is the $v - i$ characteristic of the nonlinear resistor N_R with a slope equal to G_a in the inner region and G_b in the outer region. A typical $v - i$ characteristic of N_R is shown in Fig. 5.1(b). By using the following parameters and variables:

$$\begin{cases} \tau = \dfrac{1}{RC_2}t, \alpha = \dfrac{C_2}{C_1}, \beta = \dfrac{C_2}{L} \\ x_k = \dfrac{v_{1k}}{E}, y = \dfrac{v_{2k}}{E}, z = \dfrac{R}{E}i_{3k} \end{cases}, \tag{4.3}$$

the normalized circuit equations are given as:

$$\begin{cases} \dfrac{dx_k}{d\tau} = \alpha\left\{(y_k - x_k) - Rf(x_k) + \dfrac{R}{r}(\sum_{i=1}^{N} x_i - Nx_k)\right\} \\ \dfrac{dy_k}{d\tau} = x_k - y_k + z_k \\ \dfrac{dz_k}{d\tau} = -\beta R^2 y_k \end{cases}. \tag{4.4}$$

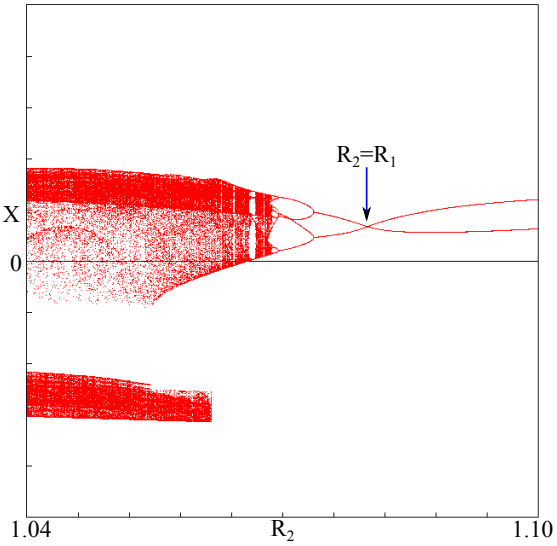

(a)

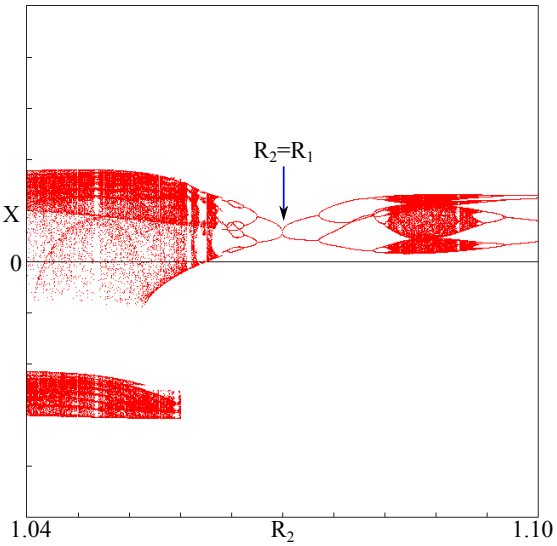

(b)

Figure 4.3 One-parameter bifurcation diagrams for the fixed parameters $\alpha = 3.7, \beta = 4.5, G_a = -1.3$ and $G_b = -0.6$ and variant R_2. (a) $R_1 = 1.08$. (b) $R_1 = 1.07$

4.3 Bifurcation analysis in the non-coupled system

We investigate bifurcations in the non-coupled parametrically forced Chua's circuit by carry out computer simulations with fourth-order Runge-Kutta method when parameters are set as $\alpha = 3.7, \beta = 4.5, G_a = -1.3$ and $G_b = -0.6$. Figure 4.3 shows one-parameter bifurcation

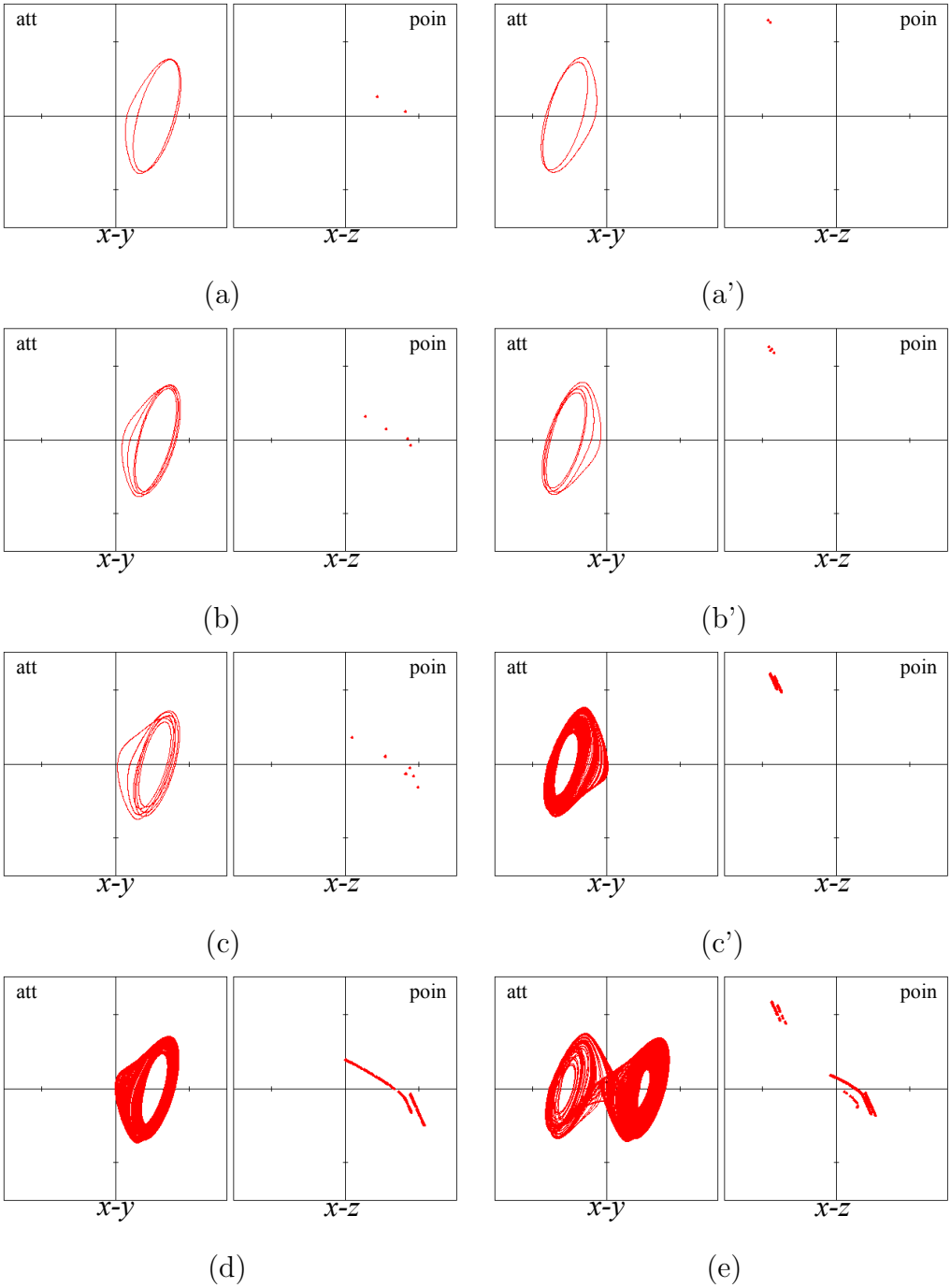

Figure 4.4 Attractors observed in the computer simulations for $\alpha = 3.7, \beta = 4.5, G_a = -1.3, G_b = -0.6$ and $R_1 = 1.07$. (a)$R_2 = 1.08$. (b)$R_2 = 1.07$. (c)$R_2 = 1.056$. (d)$R_2 = 1.05$. (e)$R_2 = 1.04$.

diagrams when R_1 is fixed and R_2 varies. In Fig. 4.3(a), an order two cycle started from the right side of the figure continues to undergo flip bifurcations and the bifurcation cascade give

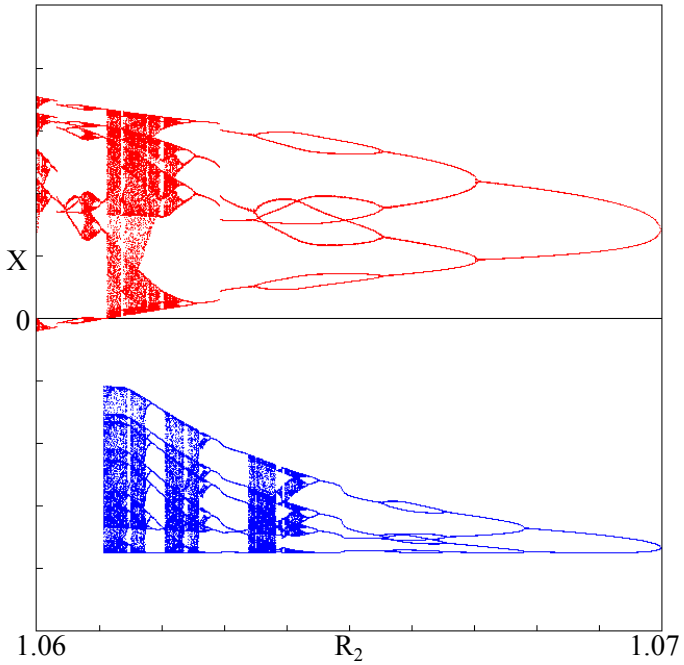

Figure 4.5 One-parameter bifurcation diagrams of coexisting attractors. The parameters are set as the same as the Fig. 4.3(b).

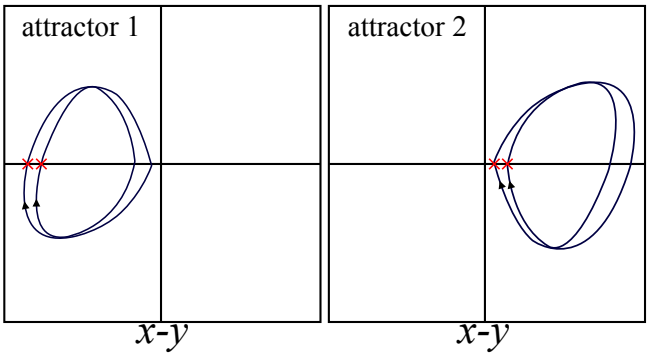

Figure 4.6 The shifting points of the switch indicated as christcross on coexisting attractors.

rise to chaos. On the cascade, an order 1 periodic cycle appears at the point $R_1 = R_2$. Except that point, all cycles are even order. In Fig. 4.3(b), the order of an cycle started from $R_1 = R_2$ increases by both of increase and decrease of R_2 when R_2 crossing through flip bifurcations. In the basic Chua's circuit, by decreasing the resistance of the linear resistor, the orders of cycles simply increase when the cycles undergo flip bifurcations. Whereas, in the parametrically forced

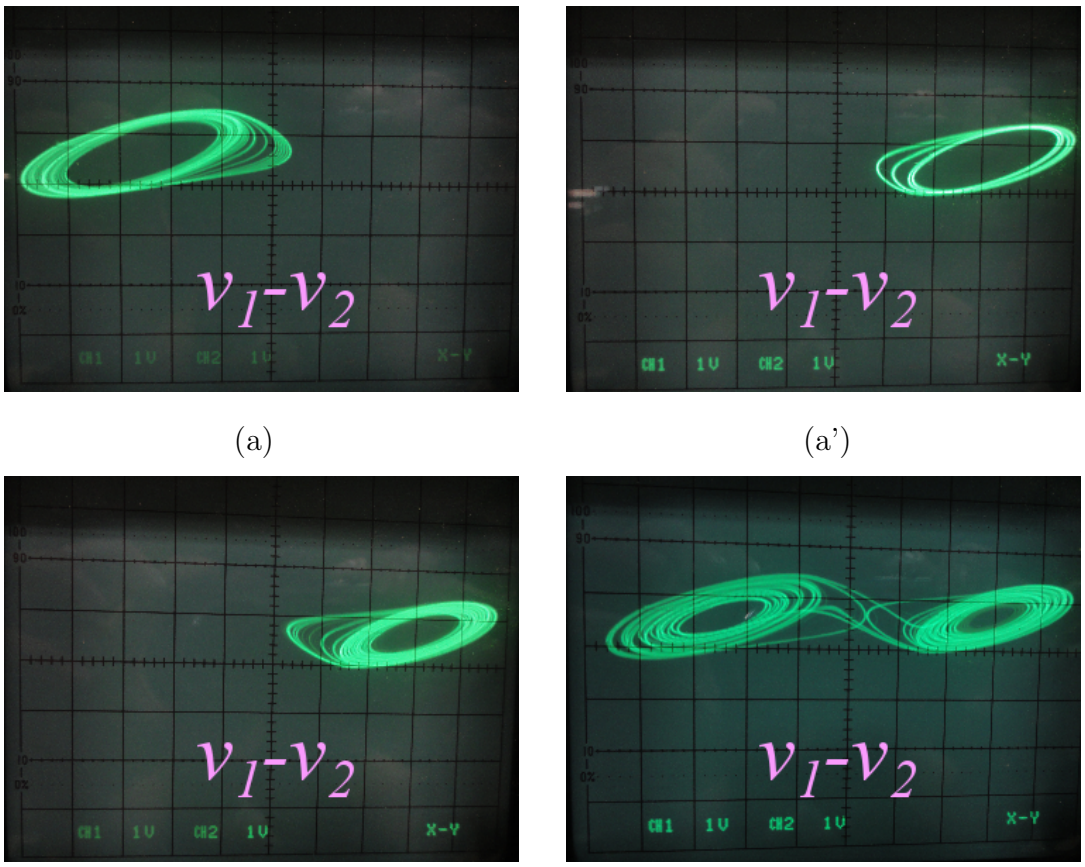

Figure 4.7 Attractors observed in the circuit experiments. $C_1 = 10nF, C_2 = 100nF, L = 18mH G_a = -0.758mS$ and $G_b = -0.409mS$. (a)$R_1 = 1.760k\Omega$ and $R_2 = 1.8555k\Omega$. (b)$R_1 = 1.752k\Omega$ and $R_2 = 1.8348k\Omega$. (c)$R_1 = 1.750k\Omega$ and $R_2 = 1.8348k\Omega$.

Chua's circuit, by decreasing R_2, the orders of cycles increase and decrease when the cycles undergo flip bifurcations.

Figure 4.4 shows attractors and their Poincaré maps on a cascade when R_1 is fixed at 1.10 and R_2 decreases. In Figs. 4.4(a) and (a'), the parameters are the same, whereas initial values are different. Two order 2 cycles coexist. By decreasing R_2, the cycles undergo a flip bifurcation and then become order 4 cycles as shown in Figs. 4.4(b) and (b'). The cycles continue to undergo flip bifurcations and then give rise to chaos. For some parameter regions, different order cycles coexist, for instance, an order 6 cycle and a chaos coexist as shown in Figs. 4.4(c) and (c'). Decreasing R_2 further, one of the coexisting attractors disappears and a

chaotic attractor remains as shown in Fig. 4.4(d). Finally, a double-scroll chaotic attractor is observed as shown in Fig. 4.4(e).

In the parametrically forced Chua's circuit, cycles which have different orders coexist such as Figs. 4.4(c) and (c'). In order to explain this phenomenon, bifurcations related to two coexisting attractors are considered. The bifurcation diagram related to two coexisting attractors are shown in Fig. 4.5. In the figure, cycles on the several cascades of bifurcations undergo flip bifurcations for different parameters. For instance, an order 2 cycle on the red colored cascade (the upper cascade) undergoes flip bifurcation at $R_2 = 1.670$ and then give rise to an order 4 cycle, whereas an order 2 cycle on the blue colored cascade (the lower cascade) undergoes flip bifurcation at $R_2 = 1.678$ and then give rise to an order 4 cycle. The switch controlling the linear resistor shifts related to the rise time of v_2, namely, the switch shifts at the points indicated by the x-marks in Fig. 4.6. The switch does not shift at symmetric points with respect to the origin on an cycle. The orbits of coexisting attractors are not symmetric with respect to the origin. Therefore, bifurcation points of the coexisting attractors are different, and there exist parameter regions where different attractors coexist.

Next, we carry out circuit experiments of the parametrically forced Chua's circuit in order to verify the observed phenomena of the computer simulations. From the investigation of the circuit experimentation, we observe the same bifurcation with the computer simulations. Of course, odd order cycles are not observed in the circuit experiments. Figure 4.7 shows attractors observed in the circuit experiment. In Figs. 4.7(a) and (a'), the parameters are the same, whereas initial values are different. It is confirmed that different attractors coexist. In Fig. 4.7(b) a single-scroll chaotic attractor is observed and no other cycles coexist. Figure 4.7(c) shows a double-scroll chaotic attractor.

4.4 Synchronization in the Two-Dimensional Coupled System

In this section, we investigate synchronizations of the two-dimensional coupled parametrically forced Chua's circuit when the parameters of the subcircuits are set as $\alpha = 3.7, \beta = 4.5, G_a = -1.3, G_b = -0.6, R_1 = 1.07$ and $R_2 = 1.0676$, and the coupling intensity r is changed. For the parameters of the subcircuits, order 2 cycle and order 4 cycle coexist in the non-coupled case.

Figure 5.3 shows attractors and phase differences observed in computer simulations. When r

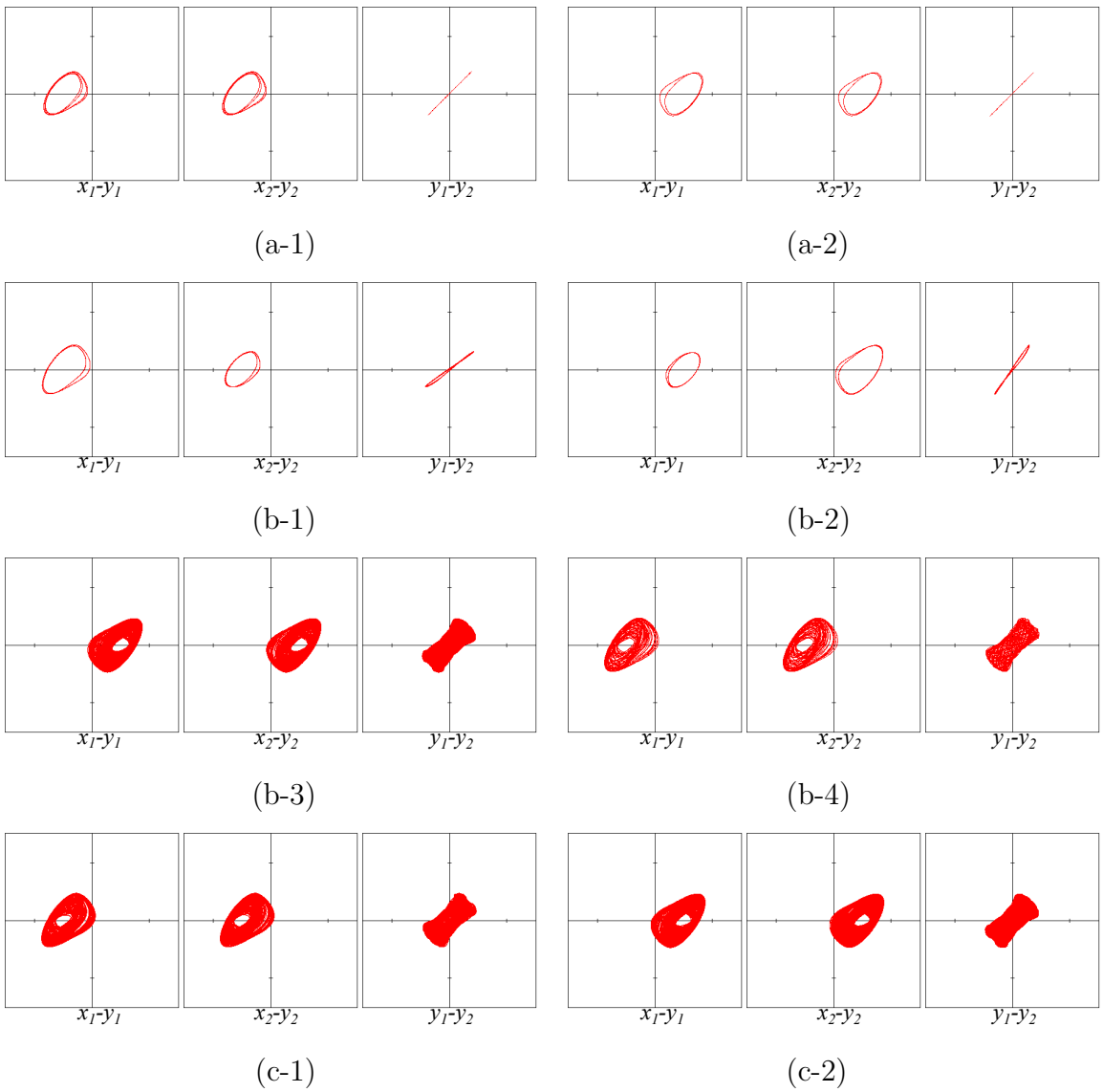

Figure 4.8 Attractors and phase differences in the coupled parametrically forced Chua's circuit. (a)$r = 4.0$. (b)$r = 6.2$. (c)$r = 6.5$.

is small, namely the coupling intensity is strong, the two subcircuits are completely synchronized at the in-phase as shown in Fig. 5.3(a). In this parameter region, two attractors, order 2 cycle and order 4 cycle, coexist. Their orders are the same as that of the attractors observed in the non-coupling case. Increasing r, the order 4 cycle undergoes a bifurcation and then give rise to order 2 cycle. In the states of the two coexisting order 2 cycles, the subcircuits are quasi-synchronized at the in-phase as shown in Figs. 5.3(b-1) and (b-2). They are almost synchronized but have little gaps in the phase difference. In this parameter region, two other attractors

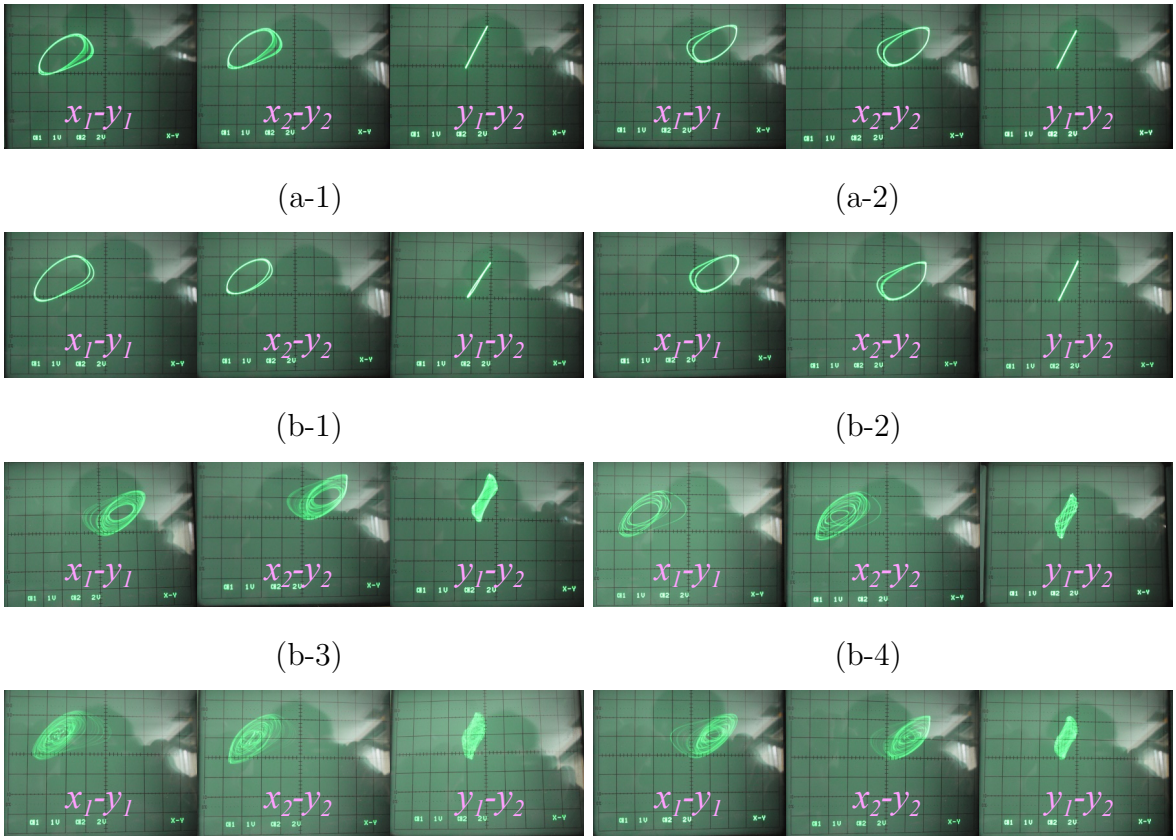

Figure 4.9 Attractors and phase differences observed in the circuit experiments. $C_1 = 10nF, C_2 = 100nF, L = 18mH G_a = -0.758mS, G_b = -0.409mS, R_1 = 1.686k\Omega$ and $R_2 = 1.7404k\Omega$. (a)$r = 1.58\Omega$. (b)$r = 11.28k\Omega$. (c)$r = 14.64k\Omega$.

coexist with other stable synchronizing states. One of the observed coexisting attractor is chaotic without synchronization as shown in Fig. 5.3(b-3). Although the attractors are high-order cycles in the figure, around this parameter region, coexisting chaotic attractors are also observed. The other coexisting attractor is high-order cycle or chaotic which is dependently changed by r, without synchronization as shown in Fig. 5.3(b-4). A total of 4 attractors coexist. Increasing r, stable states of the coexisting order 2 cycles with synchronization disappear, and the chaos without synchronization remain as shown in Fig. 5.3(c). In the parametrically forced Chua's circuit, many stable states of attractors coexist for the parameters.

Next, we carry out circuit experiments for the coupled parametrically forced Chua's circuit. Figure 4.9 shows attractors and phase differences observed in the circuit experiments.

Similar synchronization phenomena and coexistence phenomena to the results of the computer simulations are observed.

4.5 Synchronization in the Three-Dimensional Coupled System

In this section, we investigate synchronization phenomena in the three-dimensional coupled parametrically forced Chua's circuit when the parameters are set as $\alpha = 3.7, \beta = 4.5, G_a = -1.3, G_b = -0.6, R_1 = 1.07$ and $R_2 = 1.0615$.

Figure 4.10 shows attractors and phase differences between the subcircuits observed in computer simulations. In this system, many steady states coexist. However, the synchronization states are generally changed from in-phase synchronization of the all subcircuits (Fig. 4.10(a)), in-phase synchronization of two among the three subciruits (Fig. 4.10(b)) to asynchronous (Fig. 4.10(d)) for increasing of r which means weakening of the coupling intensity. Moreover, we observe interesting shift of synchronization states where two among the three subcircuits are synchronized at the quasi-in-phase sometime, although the synchronization states will be broken as time advances, after that, the synchronization states shift to another synchronization states. This phenomenon is observed a parameter region between a parameter region where two among the three subcircuits are synchronized at the in-phase and a parameter region where the subcircuits are completely asynchronous. Figure 4.11 shows the time waves of the differences between the subcircuits in the shift of synchronization states; and figure 4.12 shows attractors and phase differences when two among the three subcircuits are synchronized at the quasi-in-phase on the shift of the synchronization state. In Fig. 4.11, firstly x_1 and x_2 are synchronized at the quasi-in-phase. However, the synchronization state is broken at one point. Then, x_3 and x_1 are synchronized at the quasi-in-phase after passing of a little burst part. This shift of synchronization states continues. Here, we name the time region where two among the three subcircuits are synchronized as synchronization part, while, the time region where the subcircuits are asynchronous is named as break part.

Next, in the parameter region where the shift of synchronization states is observed, we investigate sojourn time of the synchronization part and ratio between the synchronization part and the brake part. Figures 4.13 and 4.14 show the sojourn time of synchronization part and the ratio between the synchronization part and the break part, respectively. By weakening the coupling intensity, the sojourn time become short and the ratio of synchronization part is

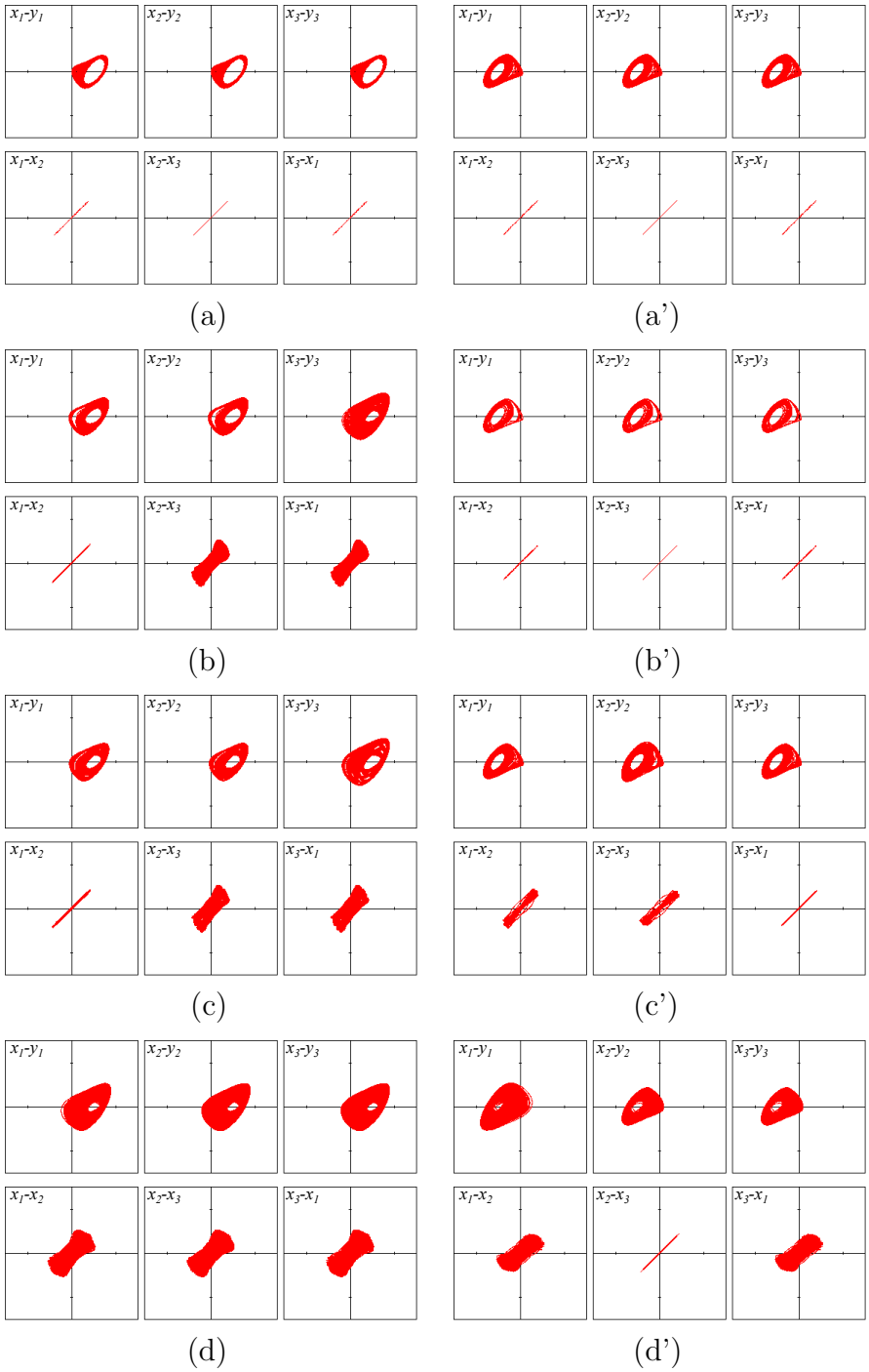

Figure 4.10 Attractors of subcircuits and phase differences between subcircuits for $\alpha = 3.7, \beta = 4.5, G_a = -1.3, G_b = -0.6, R_1 = 1.07$ and $R_2 = 1.0615$. (a) $r = 3.00$. (b) $r = 8.00$. (c) $r = 8.55$.

reduced. With weakening the coupling intensity, the rate of break part is increased and finally the synchronization state becomes asynchronous.

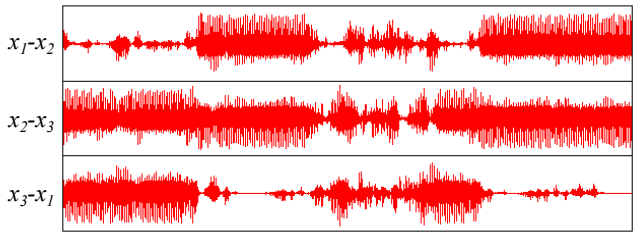

Figure 4.11 Time wave forms of the differences between the subcircuits for $\alpha = 3.7, \beta = 4.5, G_a = -1.3, G_b = -0.6, R_1 = 1.07,\ R_2 = 1.0615$ and $r = 8.55$.

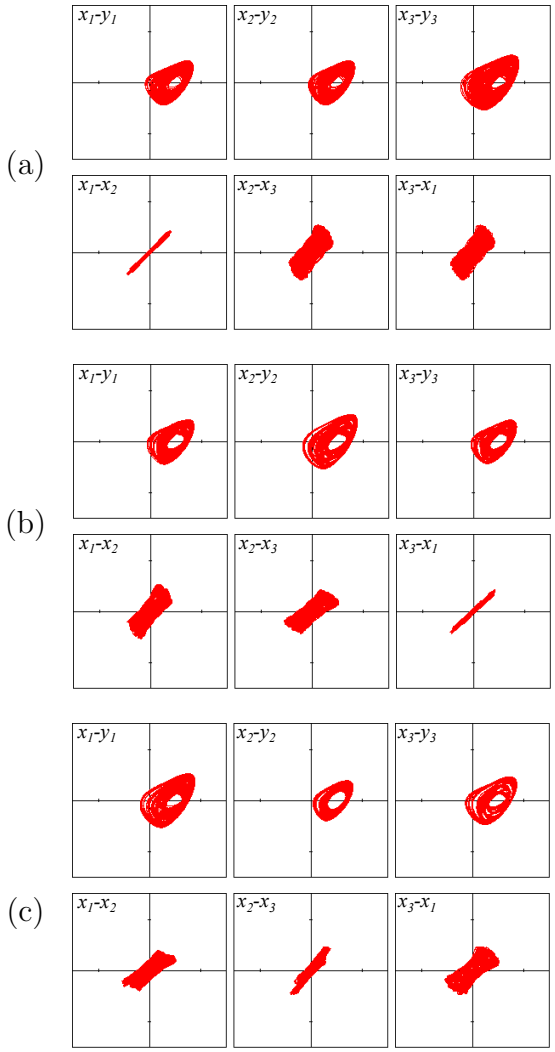

Figure 4.12 Attractors and phase differences when two among the three subcircuits are quasi synchronized on the synchronous shift of quasi-synchronization of two among the three subcircuits.

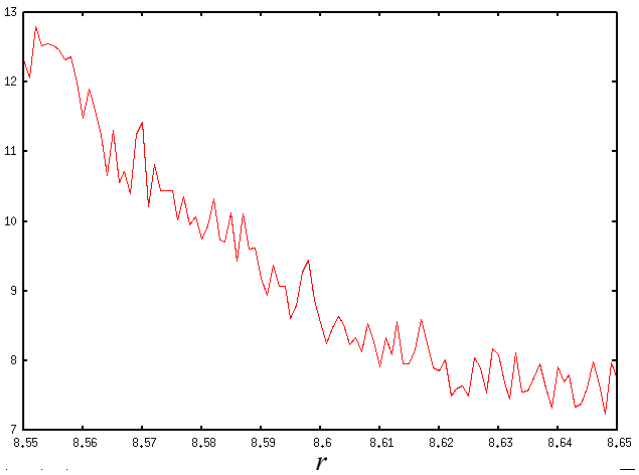

Figure 4.13 Sojourn time of synchronization part . The vertical axis is a period.

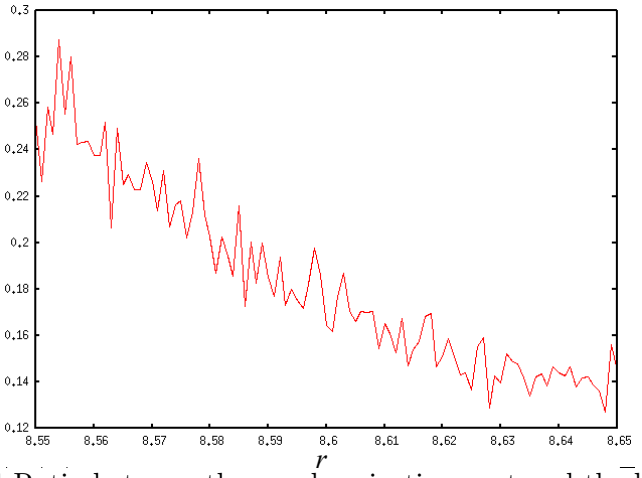

Figure 4.14 Ratio between the synchronization part and the break part.

In the same parameter region, we obtain another shift of synchronization states where two subcircuits are completely and infinitely synchronized at the in-phase whereas the remain subcircuit is not completely synchronized with the others. The remain subcircuit is synchronized with the others at the quasi-in-phase sometime, although the synchronization state will be broken as time advances, and then, the remain subcircuit become asynchronous with the others, after that, the remain subcircuit is synchronized with the others again. This shift infinitely continues. Figure 4.15 shows the time waves of the differences between the subcircuits in the shift of synchronization states; figure 4.16 shows attractors and phase differences between the subcircuits when one subcircuit is not synchronized with the others (Fig. 4.16(a)) and when one subcircuit is quasi synchronized with the others (Fig. 4.16(b)). This synchronous shift coexist with the other obtained synchronous shift.

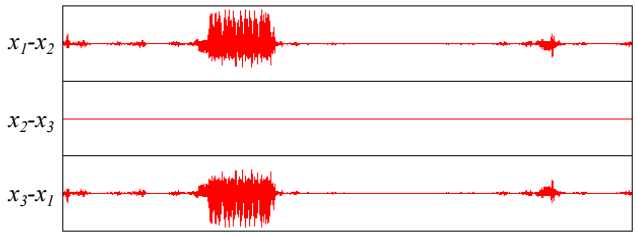

Figure 4.15 Time wave forms of the differences between the subcircuits for $\alpha = 3.7, \beta = 4.5, G_a = -1.3, G_b = -0.6, R_1 = 1.07,\ R_2 = 1.0615$ and $r = 8.55$ when the synchronous shift of quasi synchronization of one subcircuit with the others is observed.

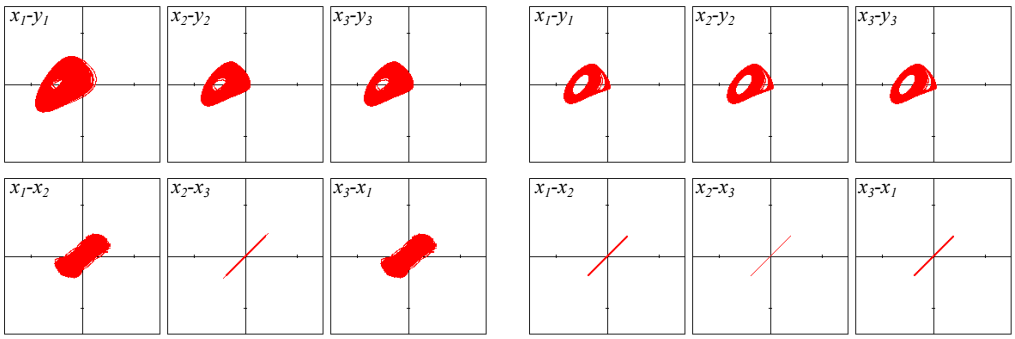

(a) (b)

Figure 4.16 Attractors and phase differences for different synchronization states on the synchronous shift of quasi synchronization of one subcircuit with the others.

4.5.1 Comparison with A Parametrically Forced Discrete-Time System

Bifurcations in a parametrically forced logistic map whose parameter is forced into periodic varying are investigated in the previous chapter. In the map, the parameter controlling nonlinearity of the logistic map alternately changes from a value to another value every step. For that periodicity, odd order cycles do not exist. The parametrically forced Chua's circuit has similar structure to the parametrically forced logistic map. The linear resistor of Chua's circuit is alternately changed from R_1 to R_2 depending on the period of y. When it is assumed that the parametrically forced Chua's circuit is discretized in association with the period of y, the parameter of the system is changed every step. This periodically change of the parameter is the same as that of the parametrically forced logistic map. In the parametrically forced

Chua's circuit non-existence of odd-order cycle is confirmed. Moreover, similar bifurcations are confirmed. An example of bifurcation diagrams in the parametrically forced logistic map is shown in Fig. 3.4 of the previous chapter. In the basic logistic map, the order of a cycle simply increases for flip bifurcations by increasing the parameter. However, in Fig. 3.4, the order of a cycle does not simply increase for flip bifurcations by increasing the parameter. Sometimes the order of the cycle decreases for flip bifurcations. For instance, an order 8 cycle undergoes a flip bifurcation at $\alpha \simeq 2.3$ and then gives rise to an order 4 cycle. Similar bifurcations are confirmed in the parametrically forced Chua's circuit as shown in Fig. 4.5.

Similar phenomena are confirmed between the parametrically forced logistic map and the parametrically forced Chua's circuit. Some phenomena in the parametrically forced logistic map are analyzed. Thus, phenomena depending on the structure of the parametric force can be analyzed by using discrete-time systems. To analyze phenomena in discrete-time systems is easier than that in continuous-time systems.

4.6 Conclusion

In this chapter, we proposed the coupled Chua's circuit whose parameter is forced into periodic varying in associated with the period of the variable. Firstly, we have investigated bifurcations in the non-coupled parametrically forced Chua's circuit by carrying out computer simulations and circuit experiments. Non-existence of odd-order cycles has been confirmed in this system. Moreover, different attractors which are not symmetric about the origin coexist, whereas, in the basic Chua's circuit, two attractors which are symmetric about the origin coexist. The cause for the coexistence of different attractors have been explained. These phenomena are also observed in the parametrically forced logistic map as shown in Chap. 3 and are caused by the structures of periodic varying of parameters in the parametrically forced systems. It is worth noting that this facilitates to analyze parametrically forced continuous-time systems, because to analyze discrete-time systems is easier than continuous-time systems. We have explained that the coexisting attractors were not symmetric with respect to the origin due to the motion of the switch in Sec. 4.3. Next, we have investigated synchronization phenomena in the coupled parametrically forced Chua's circuit. Coexistence of many attractors whose synchronization states are different have been confirmed. In the brain, neurons can have many states by the forces of ion currents and execute processing of complex information. Hence, the

investigation of parametrically forced systems can contribute to clarify information processing mechanism of the brain in future.

Chapter 5

Parametrically Forced Chua's Circuit with Independent Forces

5.1 Introduction

In this chapter, we investigate behaviors of the coupled parametrically forced Chua's circuits explained in the previous chapter, although the motion of the switches controlling R is different from the switches in the previous chapter. Each of the switches changes associated with a state value of the own subcircuit.

In the next section, we explain the coupled parametrically forced Chua's circuit. In section 3, we consider the case of two parametrically forced Chua's circuits are coupled. Coexisting of many attractors whose synchronizations states are different are observed. In section 4, we consider the case of three parametrically forced Chua's circuits are coupled. The last section is devoted to the conclusion.

5.2 Parametrically forced Chua's circuit

We consider a coupled continuous-time system whose parameter is forced into periodic varying. Chua's circuit is used as the continuous-time system. The Chua's circuits are coupled via resistors. The circuit model of the coupled system is shown in Fig. 5.1. The linear resistors of the Chua's circuits alternately changes from R_1 to R_2 depending on $v_{2k}(k = 1, 2, 3)$. The switches which cause periodic varying of the resistors are controlled by v_{2k}. Namely, the switch of each of the subcircuits is controlled by the state value of each subcircuit. The switches shift when v_{2k} is equal to 0 and changes from negative value to positive value. Figure 5.2 shows the relationship between v_{21} and the motion of the switch. The linear resistor are changed every one period of v_{2k}.

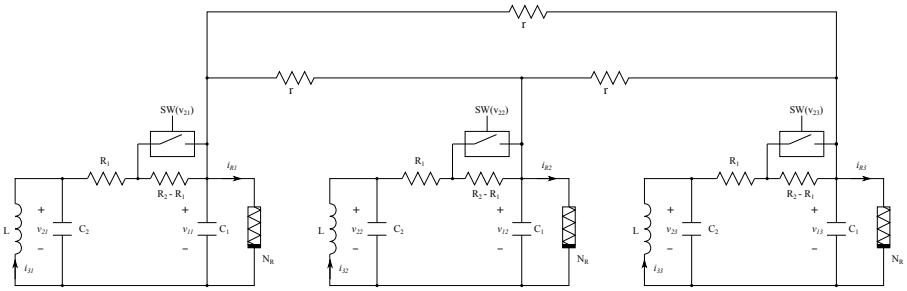

(a)

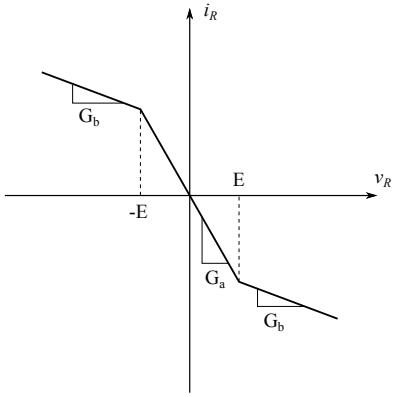

(b)

Figure 5.1 The circuit model of the parametrically forced Chua's circuit and the $i - v$ characteristics of the nonlinear resistor N_R.

The state equations of the parametrically forced Chua's circuit are:

$$\begin{cases} \dfrac{dv_{1k}}{dt} = \dfrac{1}{C_1}\left\{\dfrac{1}{R}(v_{2k} - v_{1k}) - f(v_{1k}) + \dfrac{1}{r}(\sum_{i=1}^{N} v_{1i} - Nv_{1k})\right\} \\ \dfrac{dv_{2k}}{dt} = \dfrac{1}{C_2}\left\{\dfrac{1}{R}(v_{1k} - v_{2k}) + i_{3k}\right\} \\ \dfrac{di_{3k}}{dt} = -\dfrac{1}{L}v_{2k} \\ (k = 1, 2, ..., k) \end{cases}, \tag{5.1}$$

where, R alternately changes from R_1 to R_2 depending on v_{2k}; and

$$f(v_{1k}) = G_b v_{1k} + \frac{1}{2}(G_a - G_b)\{|v_{1k+}E| - |v_{1k} - E|\} \tag{5.2}$$

is the $v - i$ characteristic of the nonlinear resistor N_R with a slope equal to G_a in the inner region and G_b in the outer region. A typical $v - i$ characteristic of N_R is shown in Fig. 5.1(b).

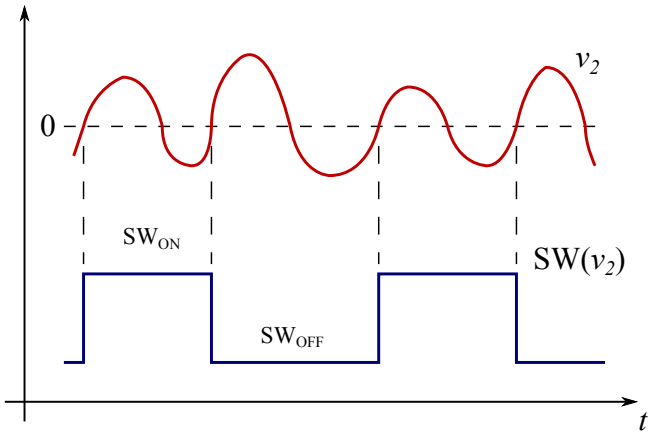

Figure 5.2 The motion of the switch depending on v_2.

By using following parameters and variables:

$$\begin{cases} \tau = \dfrac{1}{RC_2}t, \alpha = \dfrac{C_2}{C_1}, \beta = \dfrac{C_2}{L} \\ \\ x_k = \dfrac{v_{1k}}{E}, y = \dfrac{v_{2k}}{E}, z = \dfrac{R}{E}i_{3k}, \end{cases} \tag{5.3}$$

the normalized circuit equations are given as:

$$\begin{cases} \dfrac{dx_k}{d\tau} = \alpha\left\{(y_k - x_k) - Rf(x_k) + \dfrac{R}{r}(\sum_{i=1}^{N} x_i - Nx_k)\right\} \\ \\ \dfrac{dy_k}{d\tau} = x_k - y_k + z_k \\ \\ \dfrac{dz_k}{d\tau} = -\beta R^2 y_k \end{cases} . \tag{5.4}$$

5.3 Synchronization in the Two-Dimensional Coupled System

In this section, we investigate coexistence of attractors observed in two coupled parametrically forced Chua's circuits when the parameters are set as $\alpha = 3.7, \beta = 4.5, G_a = -1.3, G_b = -0.6, R_1 = 1.07$, $R_2 = 1.0676$ and $r = 4.0$. For the parameters of the subcircuits, order 2 cycle and order 4 cycle coexist in the non-coupled case.

Figure 5.3 shows attractors and phase differences observed in computer simulations. Four attractors coexist as shown in Fig. 5.3(a). Three of the four coexisting attractors are order 2 cycles, and the remain coexisting attractor is order 4 cycle. In any case of the coexisting attractors, the two subcircuits are synchronized at the in-phase. Here, we focus on the motions of the switches. We can see that there are two pattern of the motion of the switch that the two switches shift at the in-phase and the opposite-phase. By increasing r, the coupling

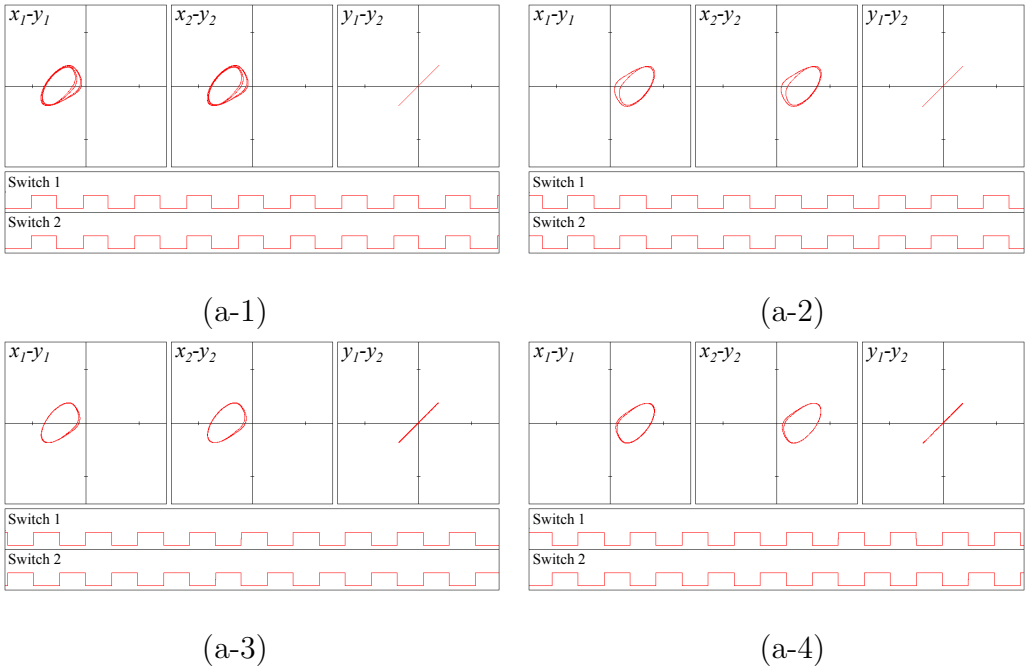

Figure 5.3 Attractors and phase differences in the coupled parametrically forced Chua's circuit. (a) $r = 4.0$. (b) $r = 6.0$.

intensity becomes weak. When $r = 6.0$, six attractors coexist as shown in Fig. 5.3(b). Two of the coexisting attractors are order 2 cycles (Fig. 5.3(b-1) and (b-2)). In this situation, the subcircuits are quasi-synchronized at the in-phase and the switches shift at the in-phase. In this parameter region, two other coexisting attractors are observed although the switches shift at the in-phase (Fig. 5.3(b-3) and (b-4)). The two attractors are chaos and the subcircuits are not synchronized. The other coexisting attractors are high-order cycles (Fig. 5.3(b-5) and (b-6)). In this situation, the subcircuits are not synchronized and the switches shift at the opposite-phase. We observed coexistence of lot of attractors. By the coupling, the motions of the switches are attracted at the in-phase or the opposite-phase. For the motions of the switches, lots of stable states are constructed.

Figure 5.4 shows basins on (x_1, z_1) phase plane when $y_1 = 0$ and $(x_2, y_2, z_2) = (0.3828, 0, 0.485)$ which is a coordinate of the orbit shown in Fig. 5.3(2). In the figure, red, blue, yellow and green colored regions correspond that the trajectories started from those regions converge the attractors shown in Fig. 5.3(1), (2), (3) and (4), respectively. Geometric patterns are presented fractal structures are confirmed.

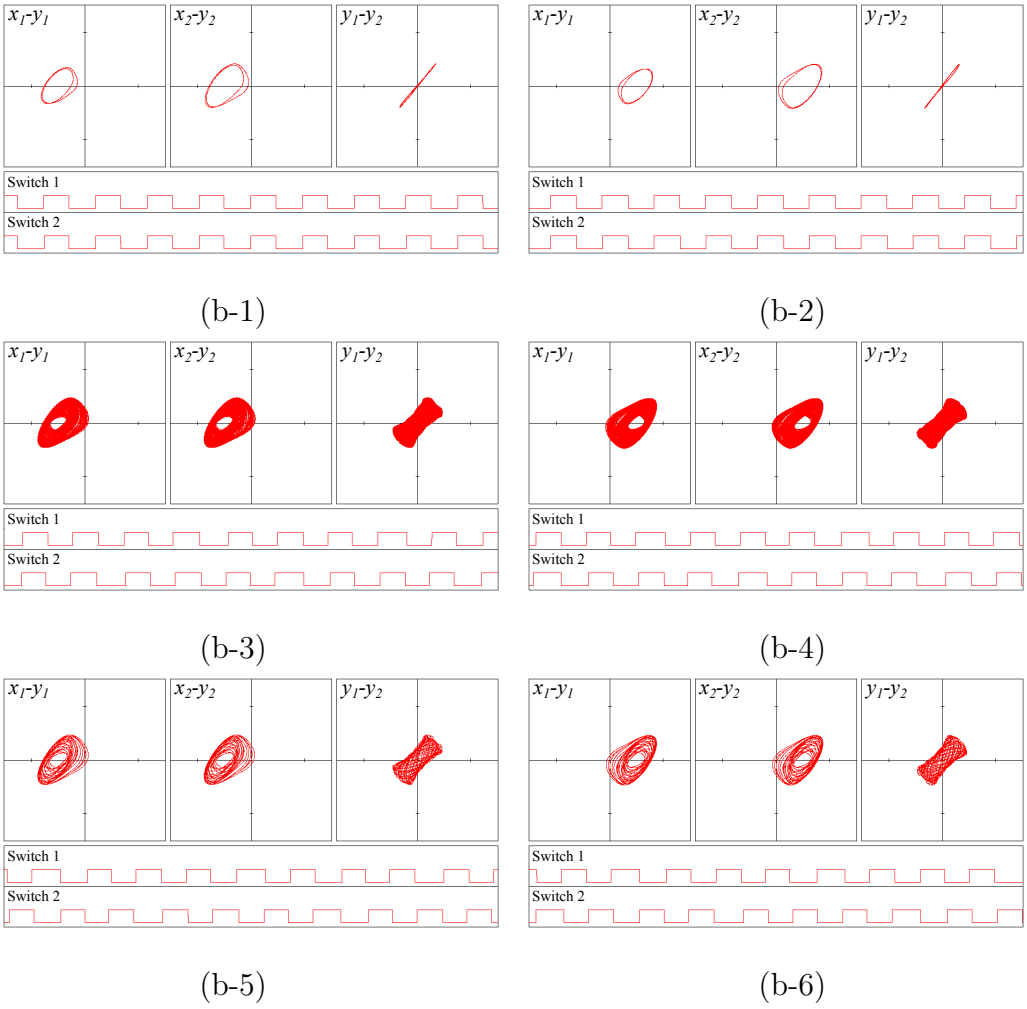

Figure 5.3 *Continued*

5.4 Synchronization in the Three-Dimensional Coupled System

In this section, we investigate synchronization phenomena in the three-dimensional coupled parametrically forced Chua's circuit when the parameters are set as $\alpha = 3.7, \beta = 4.5, G_a = -1.3, G_b = -0.6, R_1 = 1.07$ and $R_2 = 1.0615$.

Figure 5.5 shows attractors, phase differences between the subcircuits and the motion of the switches observed in computer simulations. When $r = 6.0$, eight attractors coexist as shown in Figs. 5.5(a-1)-(a-8). For this parameter, the motions of the switches are synchronized at the in-phase or the opposite-phase. When the all switches are synchronized at the in-phase, the attractors of all subcircuits are the same and synchronized at the in-phase as shown in Figs. 5.5(a-1) and (a-5). On the other hand, when one switch is synchronized at the opposite-phase with the others which are synchronized at the in-phase, six steady states are observed

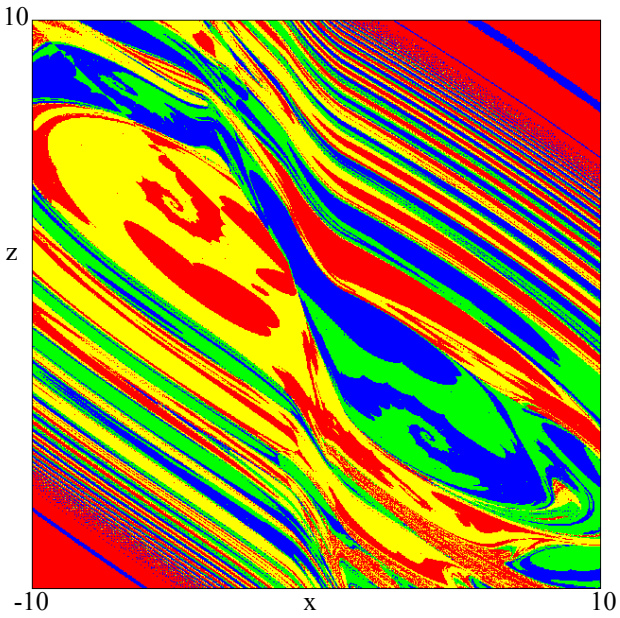

(a)

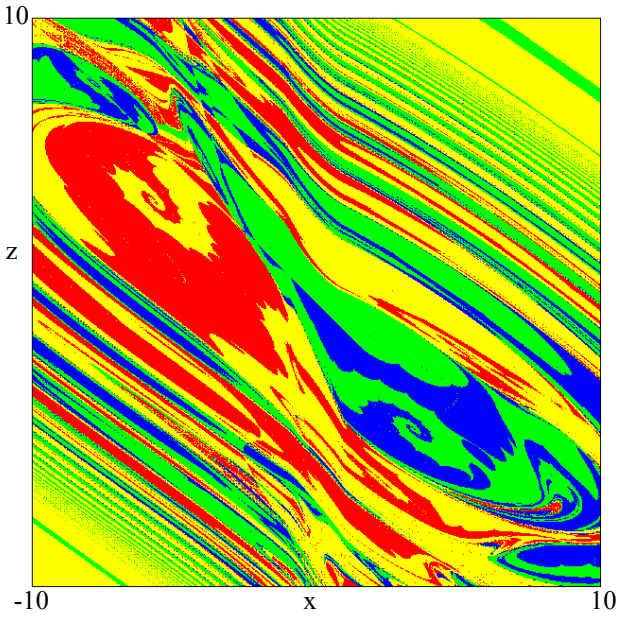

(b)

Figure 5.4 Basins on (x_1, z_1) phase plane when $y_1 = 0$. (a) $(x_2, y_2, z_2) = (0.3828, 0, 0.485)$. (b) $(x_2, y_2, z_2) = (0.849, 0, 0.214)$

in association with the synchronous states of the switches as shown in Figs. 5.5(a-2)-(a-4) and (a-6)-(a-8). In these six coexisting steady state, two subcircuits are synchronized at the in-

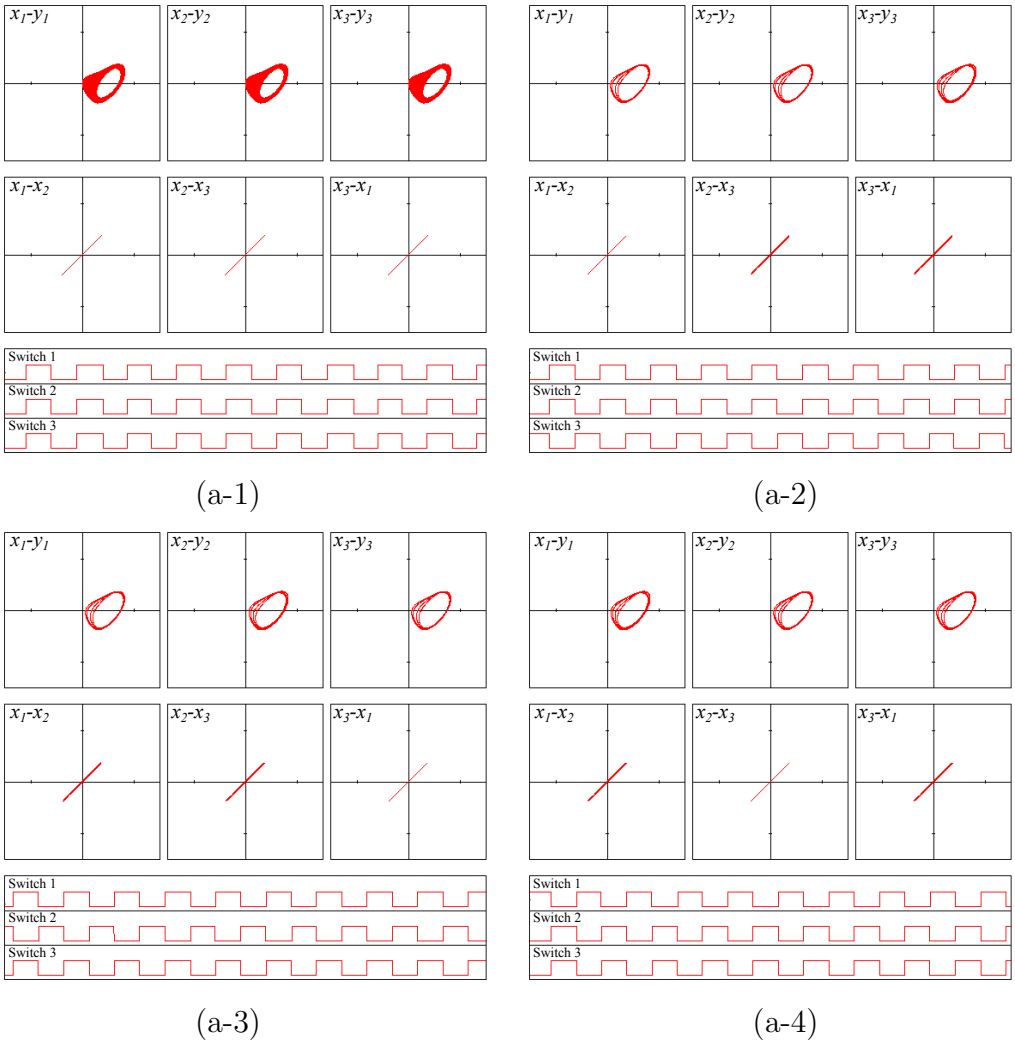

Figure 5.5 Attractors and phase differences in the coupled parametrically forced Chua's circuit. (a) $r = 6.0$. (b) $r = 9.0$.

phase and the two subcircuits are synchronized with the remain subcircuit at the quasi-in-phase. When $r = 9.0$, twelve attractors coexist as shown in Figs. 5.5(b-1)-(b-12). In this parameter, the all switches are not synchronized at the in-phase, completely. In Figs. 5.5(b-1)-(b-3), and also (b-7)-(b-9), two switches are synchronized at the in-phase and the two switches are synchronized at the quasi-in-phase with the remain switch. Then, two subcircuits are synchronized at the in-phase and the two subcircuits are synchronized with the remain subcircuit at the quasi-in-phase. Moreover, In the same of the case of $r = 6$, when one switch is synchronized at the opposite-phase with the other switches which are synchronized at the in-phase, six steady states are observed in association with the synchronous states of the switches as shown Figs. 5.5(b-

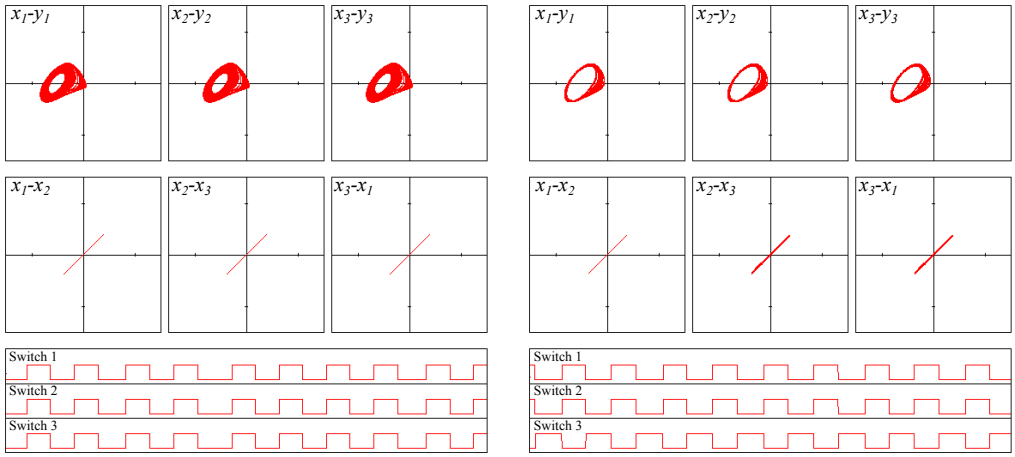

(a-5) (a-6)

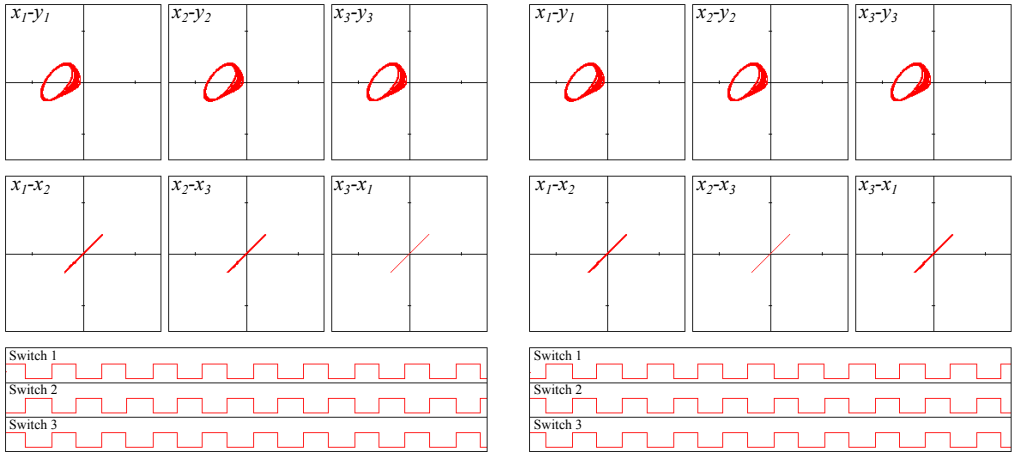

(a-7) (a-8)

Figure 5.5 *Continued*

4)-(b-6) and (b-10)-(b-12). Lots of stable states coexist.

5.5 Conclusion

In this chapter, we investigated synchronization in two identical coupled Chua's circuits whose parameters periodically varying associated with the period of internal state values of respective subcircuits. For the periodically varying of the parameters, odd-order cycles do not exist in this system. We have confirmed coexistence of lots of attractors which have different orders of cycles and different synchronization states. By the coupling, the motions of the switches are attracted at the in-phase or the opposite-phase. Then, the motions of the switches cause lots of stable states.

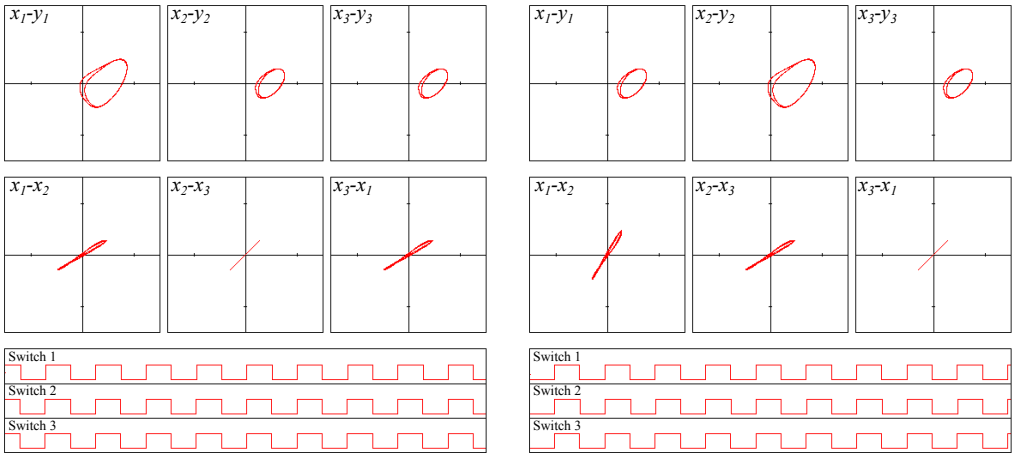

(b-1)

(b-2)

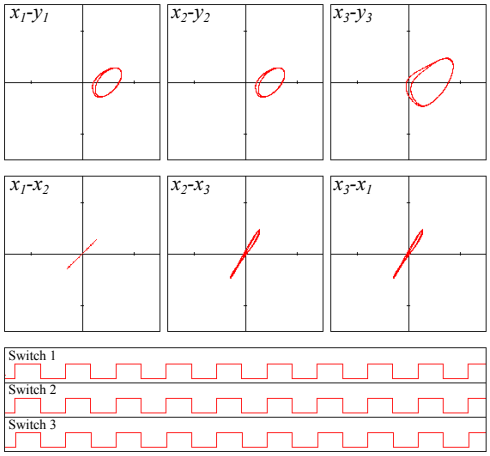

(b-3)

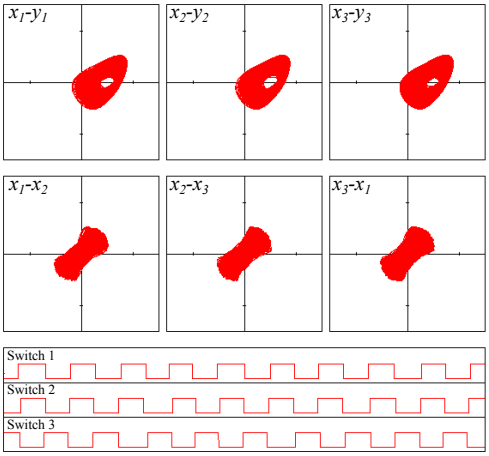

(b-4)

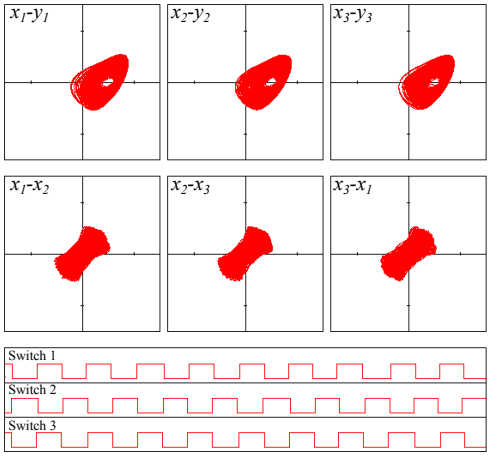

(b-5)

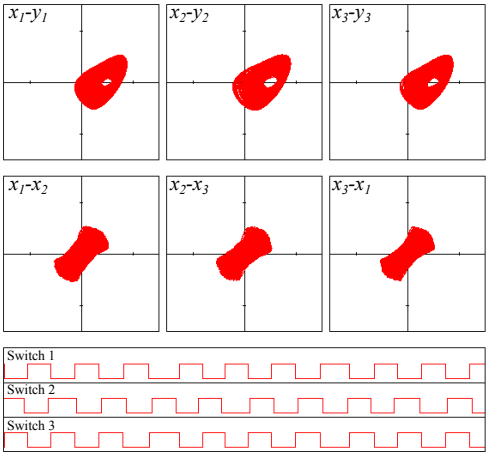

(b-6)

Figure 5.5 *Continued*

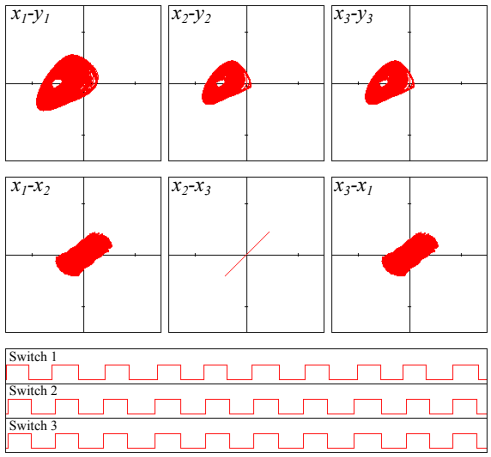

(b-7)

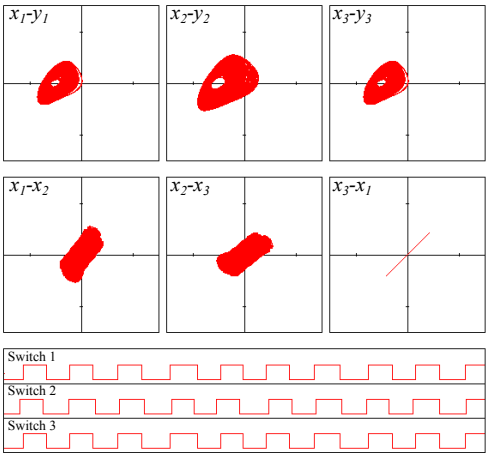

(b-8)

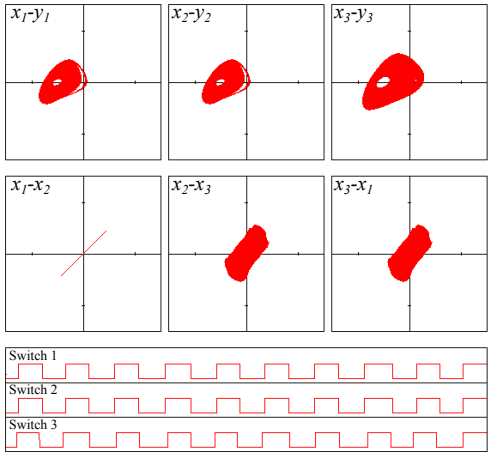

(b-9)

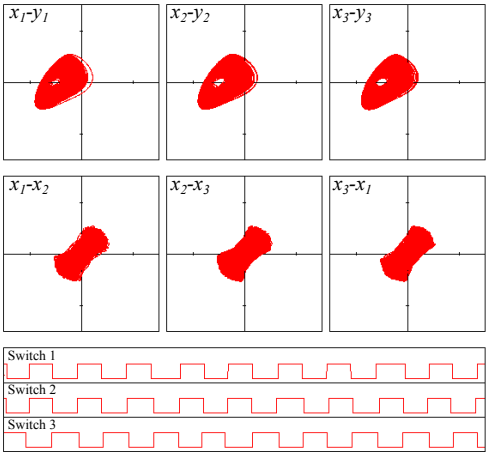

(b-10)

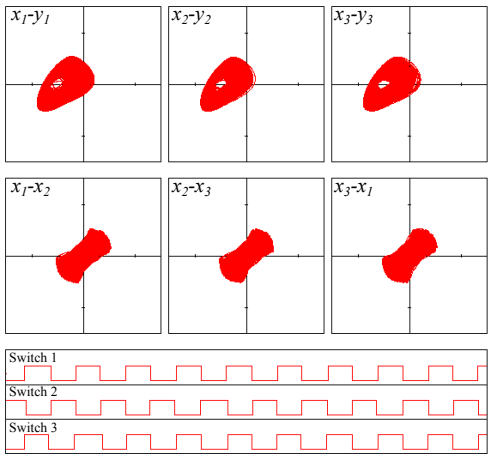

(b-11)

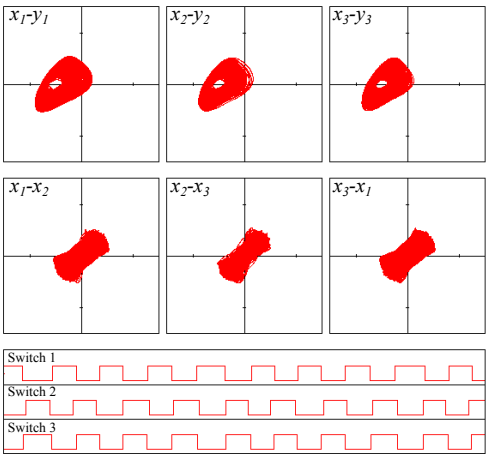

(b-12)

Figure 5.5 *Continued*

Chapter 6

Overall Conclusion

In this thesis, we proposed a N-dimensional coupled discrete-time system whose parameters are forced into periodic varying, the N-dimensional system being constructed of n same one-dimensional subsystems with mutually influencing coupling and also coupled continuous-time system including periodically parameter varying which correspond to the periodic varying in the discrete-time system.

In chapter 3, we introduced the N-dimensional coupled parametrically forced system and its general properties. Then, when logistic maps is used as the one-dimensional subsystem constructing the system, bifurcations in the one or two-dimensional parametrically forced logistic map ware investigated. Crossroad area centered at fold cusp points regarding several order cycles are confirmed.

In chapter 4, we investigated behaviors of the coupled Chua's circuit whose parameter is forced into periodic varying in associated with the period of an internal state. From the investigation of bifurcations in the system, non-existence of odd order cycles and coexistence of different attractors are observed. From the investigation of synchronizations coexisting of many attractors whose synchronizations states are different are observed. Finally, observed phenomena in the system is compared with a parametrically forced discrete-time system. Similar phenomena are confirmed between the parametrically forced discrete-time system and the parametrically forced Chua's circuit.

In chapter 5, we investigated behaviors of the coupled parametrically forced Chua's circuits explained in the previous chapter, although the motion of the switches controlling R is different from the switches in the previous chapter. Coexisting of many attractors whose synchronizations states are different are observed.

Bibliography

[1] Fujisaka, H. and Yamada, T., "Stability theory of synchronized motion in coupled-oscillator systems", *Prog. Theor. Phys.*, vol. 69, pp. 32 ☒ 47, 1983.

[2] Pecora, L. M. and Carroll, T. L., "Synchronization in chaotic systems", *Phys. Rev. Lett.*, vol.=64, pp. 821 ☒ 824, 1990.

[3] Abramson, G. and Kenkre, V. M. and Bishop, A. R., "Analytic Solutions for Nonlinear Waves in Coupled Reacting Systems", *Physica A: Statist. Mech. Appl.*, vol. 305, pp. 427 ☒ 436, 2002.

[4] Lind, P. G. and Titz, S. and Kuhlbrodt, T. and Corte-real, J. A. M. and Kurths, J. and Gallas, J. A. C. and Feudel, U., "Coupled Bistable Maps: A Tool to Study Convection Parameterization in Ocean Models", *Int. J. Bifurcation and Chaos*, vol.=14, no. 3, pp. 999-1015, 2004.

[5] Freeman, W. J., "A Neurobiological Theory of Meaning in Perception. Part I: Information and Meaning in Nonconvergent and Nonlocal Brain Dynamics", *Int. J. Bifurcation and Chaos*, vol. 13, no. 9, pp. 2493-2511, 2003.

[6] Cosp, J. and Madrenas, J. and Alarcon, E. and Vidal, E. and Villar, G., "Synchronization of nonlinear electronic oscillators for neural computation", *IEEE Trans. Neural Networks*, vol. 15, pp. 1315 ☒ 1327, 2004.

[7] Tanaka, G. and Aihara, K., "Multistate Associative Memory with Parametrically Coupled Map Networks", *Int. J. Bifurcation and Chaos*, vol. 15, no. 4, pp. 1395-1410, 2005.

[8] Kinzel, W. and Englert, A. and Reents, G. and Zigzag, M. and Kanter, I., "Synchronization of Networks of Chaotic Units with Time-Delayed Couplings", *Phys. Rev. E*, vol. 79, 056207, 2009.

[9] Lind, P. G. and Nunes, A. and Gallas, J. A. C., "mpact of Bistability in the Synchronization of Chaotic Maps with Delayed Coupling and Complex Topologies", *Physica A*, vol.=371, pp. 100-103, 2006.

[10] Schmizer, B. and Kinzel, W. and Kanter, I., "Pulses of Chaos Synchronization in Coupled Map Chains with Delayed Transmission", *Phys. Rev. E*, vol.=80, 047203, 2009.

[11] Ponce, M. and Masoller, C. and Marti, A. C., "Synchronizability of Chaotic Logistic Maps

inDelayed Complex Networks', *Phys. J. B*, vol.=67, pp. 83-93, 2009.

[12] Wang, Q. Y. and Duan, Z. S. and Perc, M. and Chen, G. R., "Pulses of Chaos Synchronization in Coupled Map Chains with Delayed Transmission", *Europhysics Lett.*, vol. 83, 50008, 2008.

[13] Wang, Q. Y. and Perc, M. and Duan, Z. S. and Chen, G. R., "Synchronization Transitions on Scale-Free Neuronal Networks Due to Finite Information Transmission Delays", *Phys. Rev. E*, vol. 80, 026206, 2009.

[14] Masoller, C. and Atay, F. M., "Complex Transitions to Synchronization in Delay-Coupled Networks of Logistic Maps", *European Phys. J D*, vol.=62, pp. 119-126, 2011.

[15] Hayashi, H. and Ishizuka, S. and Hirakawa, K., "Transition to chaos via intermittency in the Onchidium pacemaker neuron", *Phys. Lett. A*, vol. 98, pp. 474-476, 1983 (Nov.).

[16] Hayashi, C., Nonlinear Oscillations in Physical Systems, *McGraw-Hill*, Chap. 11, New York, 1964.

[17] Hayashi, C. and Abe, M. and Oshima, K. and Kawakami, H., "The Method of Mapping as Applied to the Solution for Certain Types of Nonlinear Differential Equations", *Proc. of the Ninth International Conference on Nonlinear Oscillations*, pp. 1-8, 1981 (Aug.-Sept.).

[18] Inoue, M., "A Method of Analysis for the Bifurcation of the Almost Periodic Oscillation and the Generation of Chaos in a Parametric Excitation Circuit", *Trans. of IEICE*, vol. J68-A, no. 7, pp. 621-626, 1985.

[19] Lloyd, A. L., "The Coupled Logistic Map: A Simple Model for the Effects of Spatial Heterogeneity on Population Dynamics", *J. theor. Biol.*, vol.=173, pp. 217-230, 1995.

[20] Kumeno, H. and Nishio, Y. and Fournier-Prunaret, D., "Bifurcation and Basin in Two Coupled Parametrically Forced Logistic Maps", *Proc. of IEEE International Symposium on Circuits and Systems (ISCAS'11)*, pp. 1323-1326, 2011 (May).

[21] Kawakami, H., "Bifurcations of periodic responses in forced dynamic non-linear circuits. Computation of bifurcation values of the systems parameters", *IEEE Trans. Circuits and Systems CAS-31*, pp. 248-260, 1984.

[22] Yoshinaga, T. and Kawakami, H., "Codimension two bifurcation problems in forced nonlinear circuits", *Transactions of the IEICE*, vol. E73, no. 6, 1990.

[23] Mira, C., "Chaotic Dynamics", *World Scientific Publishing Co. Pet. Ltd.*, chap. 6, Singapore, 1987.

[24] Mira, C. and Carcassès, J. P., "Crossroad area-Spring area transition (II) foliated parametric representation", *nt. J. Bifurcation and Chaos*, vol.=1, no. 3, pp. 339-348, 1991.

[25] EI Hamouly, H. and Mira, C., "Singularités dues au feuilletage du plan des bifurcations d'un difféomorphisme bi-dimensionnel", *C. R. Acar. Sc. Paris*, vol. 1294, pp. 387-390, 1982.

[26] Fournier-Prunaret, D and Kawakami, H. and Mira, C., "Feuilletage du plan des bifurcations d'un difféomorphisme bi-dimensionnel. Doublement de l'ordre des zones source et des zones échangeur", *C. R. Acad. Sc. Paris, sér.*, vol. 1301, pp. 223-226, 1985.

[27] Carcassès, J. P. and Mira, C. and Bosch, M. and Simó, C. and Tatjer, J. C., "Crossroad area-Spring area transition, (I) parameter plane representation", *Int. J. Bifurcation and Chaos*, vol. 1, no. 1, pp. 183-196, 1991.

[28] Mira, C. and Carcassès, J. P., "On the crossroad area-saddle area and crossroad area-spring area transitions", *nt. J. Bifurcation and Chaos*, vol.=1, no. 2, pp. 641-655, 1991.

[29] Carcassès, J. P., "Determination of Different Configurations of Fold and Flip Bifurcation Curves of A One or Two-Dimensional Map", *Int. J. Bifurcation and Chaos*, vol. 3, no. 4, pp. 869-902, 1993.

[30] Mira, C. and Gardini, L. and Barugola, A. and Cathala, Fean-Claude, DChaotic Dynamics in Two-Dimensional Noninvertible Maps, *World Scientific Series on Nonlinear Science. Series A, Vol. 20.*, 1996.